THE UNIVERSITY OF ALBERTA

RELEASE FORM

NAME OF AUTHOR Pratap Narayan Sahay

TITLE OF THESIS SEISMIC SOURCE THEORY

DEGREE FOR WHICH THESIS WAS PRESENTED MASTER OF SCIENCE

YEAR THIS DEGREE GRANTED Fall 1980

THE UNIVERSITY OF ALBERTA

SEISMIC SOURCE THEORY

by

© Pratap Narayan Sahay

A THESIS

SUBMITTED TO THE FACULTY OF GRADUATE STUDIES AND RESEARCH

IN PARTIAL FULFILMENT OF THE REQUIREMENTS FOR THE DEGREE

OF MASTER OF SCIENCE

IN

GEOPHYSICS

DEPARTMENT OF PHYSICS

EDMONTON, ALBERTA

Fall 1980

THE UNIVERSITY OF ALBERTA

FACULTY OF GRADUATE STUDIES AND RESEARCH

The undersigned certify that they have read, and recommend to the Faculty of Graduate Studies and Research, for acceptance, a thesis entitled SEISMIC SOURCE THEORY submitted by Pratap Narayan Sahay in partial fulfilment of the requirements for the degree of MASTER OF SCIENCE in GEOPHYSICS.

ABSTRACT

Theoretical modeling of the source region is done in order to understand the physical process occurring in the earthquake. In the beginning it was modeled as a point source, later on the fault dimension and the slip on the fault was taken into account by developing the dislocation models. Recently studies on the occurrence of an earthquake and the resultant seismic motion from nucleation of a crack, its spreading and stopping which develops under stress condition and material properties of the source region, have been started.

ACKNOWLEDGEMENTS

With sincere gratitude I wish to thank my supervisor Dr. A. Z. Capri for his help and encouragement throughout the course of this work.

To the Department of Physics I am indebted for the finanlcial support.

Also I would like to thank my colleagues in the seismology group for helpful discussions.

Table of Contents

1. INTRODUCTION

The desire to achieve some depth of understanding of the earthquake process, leads to the formulation of different models for this complex phenomenon. In seismic source theory, this theoretical modeling is studied systematically.

The theoretical study of the seismic source has traditionally been concerned with attempts to construct models that simulate the faulting process, which, dating from the early work of Reid on the great San-Fransisco earthquake of 1906, is accepted as the most valid physical description of shallow earthquakes. The first approach to the description of the faulting process of an earthquake was based on the consideration of various simple point sources and couples, within or on the surface of an elastic medium. Reviews and extensive bibliographies are given by Balakina et al. (1961) and Honda (1962) where the original work of Byerly, Hodgson, Nakano, and others is discussed.

A more elaborate model based on dislocation theory was first proposed by Volterra (1907) and later generalized and extensively applied by Steketee (1958), Maruyama (1963), Burridge and Knopoff (1964), Haskell (1964, 66, 69), and others.

The modeling of the actual physical process of the source started with Kostrov's work on self-similar cracks of the 1960's where it is described as crack propagation.

With the work of Burridge and Knopoff (1967) on the numerical simulation of the fault motion and earthquake occurrence, computer modeling of the source has started.

In chapter II and III a closer look at the theoretical nature of the seismic sources is taken. Chapter IV is devoted to the earthquake as a fracture process. The numerical simulation of earthquakes is discussed in chapter V. Reviews of the source theory can be found in Archambeau(1968,75), Ben-Menahem and Singh (1972). A summary of later work is given by Johnson (1979).

2. KINEMATICS OF THE SOURCES

An earthquake may involve non-linear processes such as brittle fracture, plastic flow, phase change and other complicated phenomena. As direct observation in the region where these processes take place (source region) is difficult, the problem is attacked by assuming some model for source region and then calculating the displacement field for such a source. The objective of this approach is to estimate the parameters characterizing the source by the inspection of the radiation field.

Inside the source region the linear equations of motion do not hold, so the displacement field can be calculated if source region is squeezed to a singularity outside which linear equations of motion are valid. In such a case the equations of motion can be solved by adding a term, usually called, the body force equivalent of the source. If the medium under consideration is isotropic and homogeneous or if the anisotropy or inhomogeneity is of simple type then one may be able to solve the equations of motion by first developing a Green's function with appropriate boundary conditions and then convolving it with the source term.

Let f_i be the source term for the earthquake process,

then the equation of motion are,

$$(C_{ijpq} u_{p,q})_{,j} - \rho \ddot{u}_i = - f_i \qquad 2.1$$

where $C_{ijpq} = \lambda \delta_{ij} \delta_{pq} + \mu(\delta_{ip}\delta_{jq} + \delta_{iq}\delta_{jp})$ is the elastic constant of the medium.

For homogeneous isotropic whole space, the retarded Green's function for the above equation with causality condition is

$$G_{ij}(\vec{x},t;\vec{x}',t') = (4\pi\rho)^{-1}\Big[(3\gamma_i\gamma_j - \delta_{ij})\, r^{-3}\int_{r/v_p}^{r/v_s} \delta(t-t'-\xi)\xi\, d\xi + \gamma_i\gamma_j (v_p^2 r)^{-1}$$

$$\cdot\, \delta(t-t'-r/v_p) - (\gamma_i\gamma_j - \delta_{ij})\,(v_s^2 r)^{-1}\, \delta(t-t'-r/v_s)\Big] \qquad 2.2$$

where

$\vec{x}$ = co-ordinate of observation point

$\vec{x}'$ = co-ordinate of source point

r = $|\vec{x} - \vec{x}'|$

γ_i = direction cosine of line from source to obs. point

= $\dfrac{(x_i - x_i')}{r}$

v_p = P wave velocity

v_s = S wave velocity

i is the component of displacement at the obs. point.

j is the direction of the force acting at the source.

Using symmetry and time translation property of the

Green's function we get

$$U_i(\vec{x},t) = \int_{-\infty}^{+\infty} dt' \Big[\int_V d^3\vec{x}'\, G_{ij}(\vec{x},t;\vec{x}',t')\, f_j(\vec{x}',t') + \int_S \nu_K\, d^2\vec{x}' \Big\{ G_{ij}(\vec{x},t;\vec{x}',t')$$

$$\cdot C_{jKpq}\, U_{p,q}(\vec{x}',t') - U_j(\vec{x}',t')\, C_{jKpq}\, G_{ip,q}(\vec{x},t;\vec{x}',t') \Big\} \Big] \qquad 2.3$$

Putting 2.2 into 2.3 and carrying out the integration with respect to t', we get

$$U_i(\vec{x},t) = \int_V G_{ij}[f_j]\, d^3\vec{x}' + \int_S C_{jKpq}\, G_{ij}[U_{p,q}]\, \nu_K\, d^2\vec{x}'$$

$$+ \frac{\partial}{\partial x_q} \int_S C_{jKpq}\, G_{ip}[U_j]\, \nu_K\, d^2\vec{x}' \qquad 2.4$$

where $G_{ij}[\phi]$ is an operator on ϕ defined as,

$$G_{ij}[\phi] = (4\pi\rho)^{-1} \Big[(3\gamma_i\gamma_j - \delta_{ij})\, r^{-3} \int_{r/v_p}^{r/v_s} \phi(\vec{x}', t-\xi)\, \xi\, d\xi + \gamma_i\gamma_j (v_p^2 r)^{-1}$$

$$\cdot \phi(\vec{x}', t - r/v_p) - (\gamma_i\gamma_j - \delta_{ij})(v_s^2 r)^{-1} \phi(\vec{x}', t - r/v_s) \Big] \qquad 2.5$$

The above equation gives the elastic displacement at any arbitary point inside a homogeneous isotropic body V enclosed by S in terms of distribution of f_i in V and the value of U_j and $U_{p,q}$ on the S_o. Now splitting S into an inner S_o (surrounding the source) and an outer

boundary S_1 of V and letting S_1 to go to infinity where homogeneous boundary conditions are satisfied, the surface integration in the equation 2.4 reduces only on S_0 .

The various earthquake source models are basically different representations of the source term f_i , the source region boundary S_0 , inside which non-linear phenomena are taking place, and the displacement and stress fields on S_0 . All theoretical source representations can be classified as:

1. Point source models
2. Dislocation models

2.1 Point source models:-

In the point source representation of the earthquakes the source region is squeezed to a point, so that the surface term is expressed as a single force or a cluster of forces localized in a squeezed source region. Therefore the expression for the displacement field in this case becomes

$$U_i(\vec{x},t) = \int_V G_{ij}\,[f_j]\,d^3\vec{x}' \qquad 2.6$$

Using the above formula, the displacement field for any

point source can be calculated.

Single Force:-

The trivial representation for a point source is a single force. The source term for a single force is

$$f_i = \hat{e}_i \, \delta_{ij} \, \delta(\vec{x}-\vec{x}') \cdot F(t) \quad . \qquad 2.7$$

$F(t)$ is the time dependent part of the force. With this we get,

$$U_i(\vec{x},t) = (4\pi\rho)^{-1}\Big[(3\gamma_i\gamma_j-\delta_{ij})\, r^{-3}\int_{r/v_p}^{r/v_s} \xi\, F(t-\xi)\, d\xi + \gamma_i\gamma_j\,(v_p^2 r)^{-1} \qquad 2.8$$

$$\cdot F(t-r/v_p) - (\gamma_i\gamma_j-\delta_{ij})\,(v_s^2 r)^{-1}\, F(t-r/v_s)\Big]$$

The first term in the equation 2.8 attenuates like r^{-3} and is called the near field term while other two terms which attenuate like r^{-1} are called the far field terms.

Near field term:-

$$U_i^N = (4\pi\rho)^{-1}(3\gamma_i\gamma_j-\delta_{ij})\, r^{-3}\int_{r/v_p}^{r/v_s} \xi\, F(t-\xi)\, d\xi \qquad 2.9$$

This can be decomposed into the terms apparently propagating with P and S waves velocities by introducing the following integral,

$$J(t) = \int_0^t d\xi \int_0^\xi F(\eta)\, d\eta \qquad 2.10$$

Integrating by parts,

$$\int_{r/v_p}^{r/v_s} \xi F(t-\xi)\, d\xi = -\frac{r}{v_s} \dot{J}(t-r/v_s) + \frac{r}{v_p} \dot{J}(t-r/v_p)$$

$$- J(t-r/v_s) + J(t-r/v_p). \qquad 2.11$$

Putting 2.11 into the equation 2.9, we find four terms like

$$r^{-3} J(t-r/v_p), \quad r^{-3} J(t-r/v_s), \quad r^{-2} \dot{J}(t-r/v_p), \quad r^{-2} \dot{J}(t-r/v_s). \qquad 2.12$$

The first term propagates with P wave velocity and attenuates as r^{-3}, with the wave proportional to a double integration of the force. Likewise, the third term also propagates with P wave velocity and attenuates as r^{-2}, with the wave proportional to one integration of the force. Similarly other two terms propagate with S wave velocity. This theoretical decomposition is elegant, but on a record all arrive at the same time or nearly at the same time so they cannot be separated. They can be distinguished only if they are observed at a long distance. But due to the fast

attenuation with distance they are negligible there.

The radial component of u_i^N is,

$$\gamma_i u_i^N = (4\pi\rho)^{-1} \; 2\gamma_j r^{-3} \int_{r/v_p}^{r/v_s} \xi F(t-\xi)\, d\xi \tag{2.13}$$

Therefore the S wave in this form will have a radial component.

Define a vector γ_i' orthonormal to γ_i

$$\gamma_i' \cdot \gamma_i = 0$$

Then the transverse component of u_i^N is,

$$\gamma_i' \cdot u_i^N = -(4\pi\rho)^{-1} \gamma_j' \, r^{-3} \int_{r/v_p}^{r/v_s} \xi F(t-\xi)\, d\xi \tag{2.14}$$

Clearly the P wave here will have a transverse component.

<u>Far field term:-</u>

The far field term has two parts, one propagates with P wave velocity while another with S wave velocity, both are proportional to the applied force and attenute as r^{-1} . The far field P term is,

$$u_i^P = (4\pi\rho)^{-1} \gamma_i \gamma_j (v_p^2 r)^{-1} F(t - r/v_p) \tag{2.15}$$

As $\gamma_i' \cdot u_i^P = 0$, the far field P term does not have a transverse component. The radial component is

$$\gamma_i u_i^P = (4\pi\rho)^{-1} \gamma_j (v_P^2 r)^{-1} F(t - r/v_P) \qquad 2.16$$

Clearly the directivity pattern is proportional to γ_j, the direction cosine of line joining source and observation points, looks like fig. 2.1a .

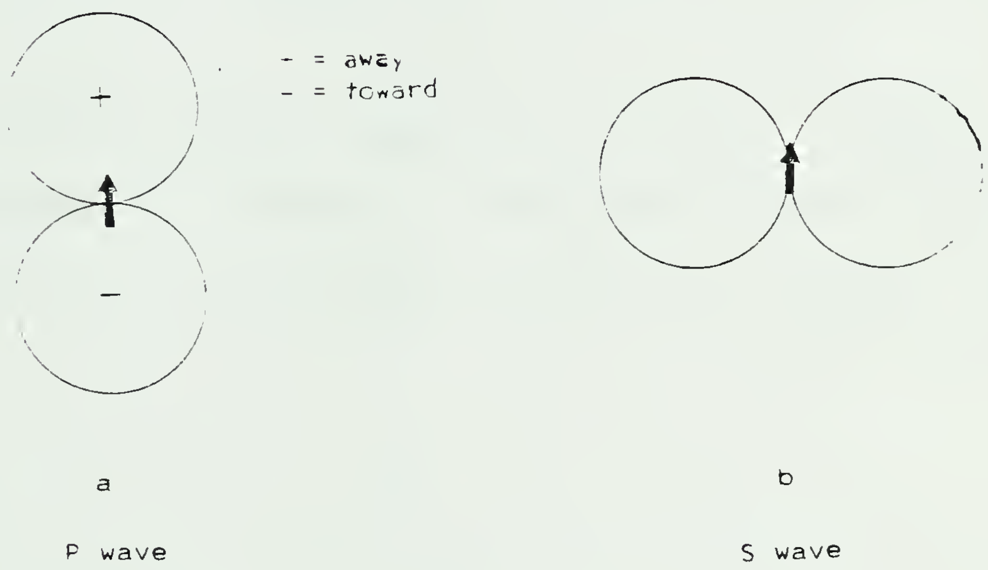

Fig. 2.1 Directivity patterns for single force.

The far field S term is

$$u_i^S = -(4\pi\rho)^{-1} (\gamma_i \gamma_j - \delta_{ij}) (v_s^2 r)^{-1} F(t - r/v_s) \qquad 2.17$$

The radial component is zero while the transverse component is

$$\gamma_i' \cdot u_i^S = (4\pi\rho)^{-1} \gamma_j' (v_s^2 r)^{-1} F(t - r/v_s) \qquad 2.18$$

Here the radiation pattern is proportional to γ_j', and looks like fig. 2.1b .

Single couple:-

The source term for a single couple due to forces acting in the j^{th} direction separated along the K^{th} direction is,

$$f_i = -\hat{e}_i \, \delta_{ij} \frac{\partial}{\partial x_K} \delta(\vec{x}-\vec{x}') \cdot F(t) \qquad 2.19$$

If $j=K$ the source term is called a single couple without moment or dipole, otherwise single couple with moment (fig. 2.2). Thus there can be three dipoles and six couples.

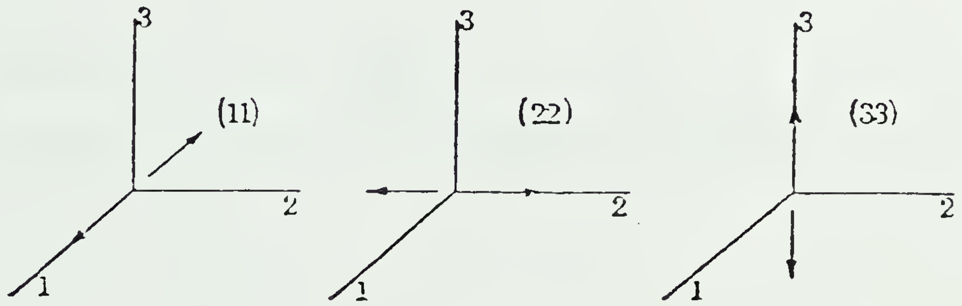

Fig. 2.2a Dipole coresspounding to (jk)=(11), (22), (33).

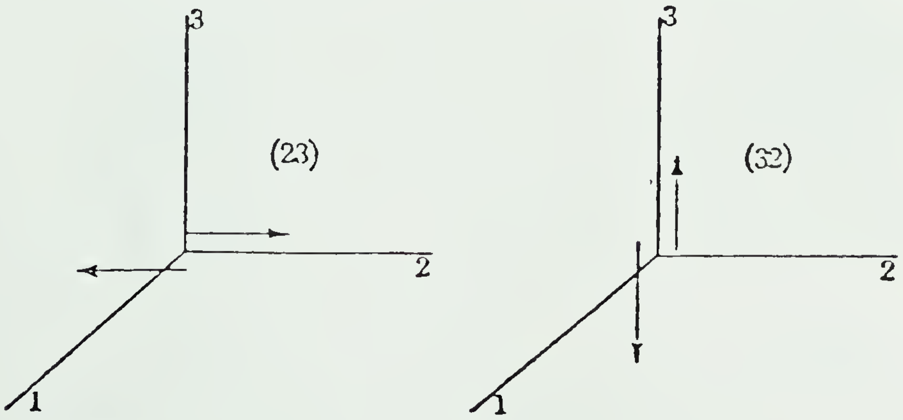

Fig. 2.2b Single couple (23) and (32).

Now the source term for a single force (equation 2.7) on differentiation w.r.t. x_K yields the source term for a single couple (equation 2.19), therefore, the solution for a single force (equation 2.8) on differentiation w.r.t. x_K will give the solution for a single couple, which is (Haskell 1963),

$$
\begin{aligned}
u_i^K = (4\pi\rho)^{-1} \Big[& \{3(\gamma_i \delta_{jK} + \gamma_j \delta_{iK} + \gamma_K \delta_{ij}) - 15\, \gamma_i \gamma_j \gamma_K\} \{ J(t - r/v_P)/r^4 \\
& + \dot{J}(t - r/v_P)/v_P r^3 - J(t - r/v_S)/r^4 - \dot{J}(t - r/v_S)/v_S r^3 \} + \{\gamma_i \delta_{jK} \\
& + \gamma_j \delta_{iK} + \gamma_K \delta_{ij} - 6 \gamma_i \gamma_j \gamma_K\}\{ \ddot{J}(t - r/v_P)/v_P^2 r^2 - \ddot{J}(t - r/v_S)/v_S^2 r^2 \} \\
& + \gamma_i \gamma_j \gamma_K \cdot \{ -\dddot{J}(t - r/v_P)/v_P^3 r \} + (\gamma_i \gamma_j \gamma_K - \gamma_K \delta_{ij})\, \dddot{J}(t - r/v_S)/v_S^3 r \Big]
\end{aligned} \qquad 2.20
$$

The directivity pattern in the far field for a dipole and a single couple with moment is shown in fig 2.3 .

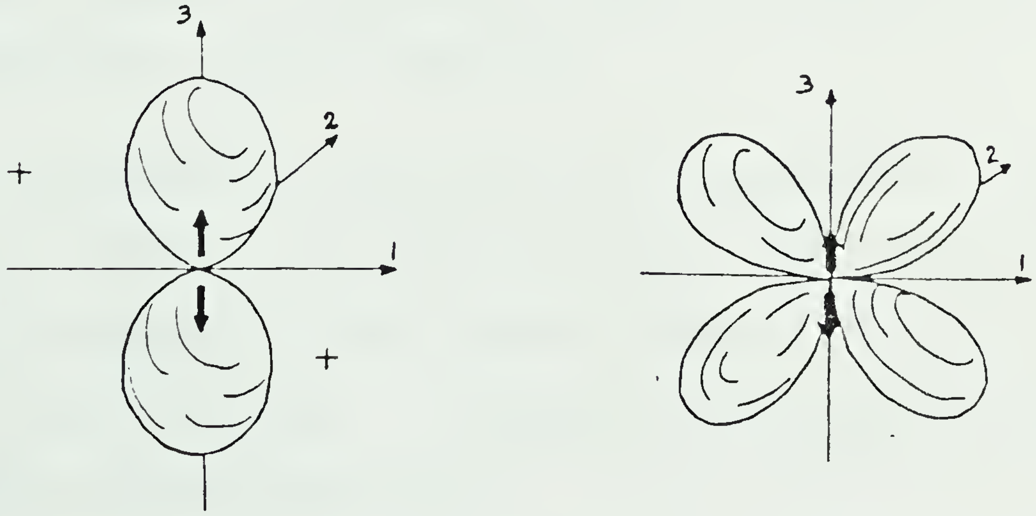

P wave   S wave

Fig. 2.3a Directivity patterns for doublet.

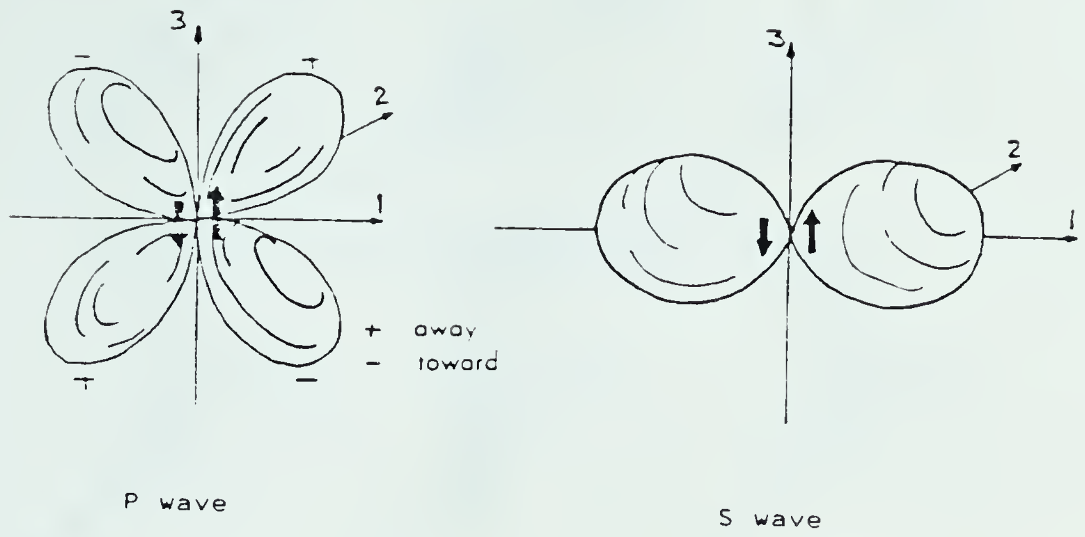

Fig. 2.3b Directivity patterns for single couple with moments

<u>Center of dilatation, Double couple and Center of rotation:-</u>

The source terms for these are linear combinations of single couple source terms.

The center of dilatation is a linear combination of three equal and mutually perpendicular dipoles.

The double couple is linear combination of two coplanar single couples of equal but opposite moments with mutually perpendicular force directions.

The center of rotation is a combination of two coplanar single couples of moment of equal magnitude acting in the same direction, so that the net moment is not zero but the net force is zero. Although, this type of source is not possible in the real earth.

The distribution of forces for all of these are shown in fig. 2.4 .

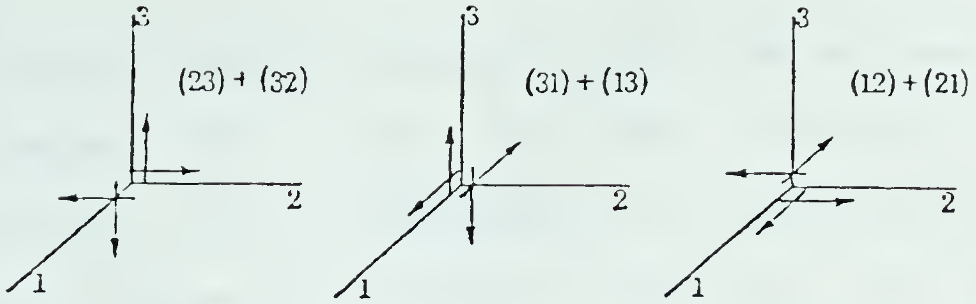

Fig. 2.4a Three fundamental double couples.

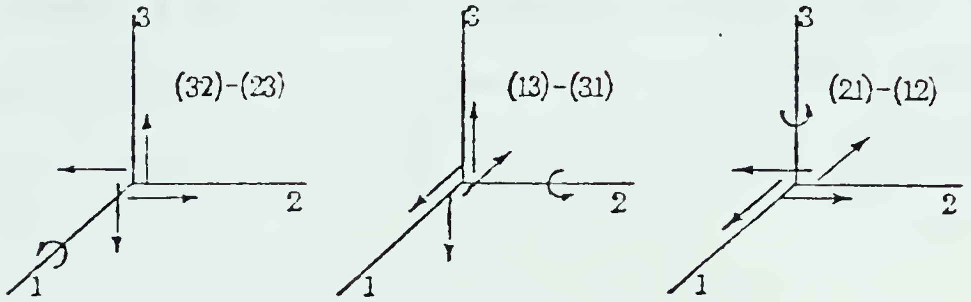

Fig. 2.4b Center of rotation with moment about x_1, x_2, and x_3 -directions.

Clearly the displacement field for each can be obtained with a proper combination of solution for single couples (equation 2.20).

The directivity pattern for each is shown in fig. 2.5 .

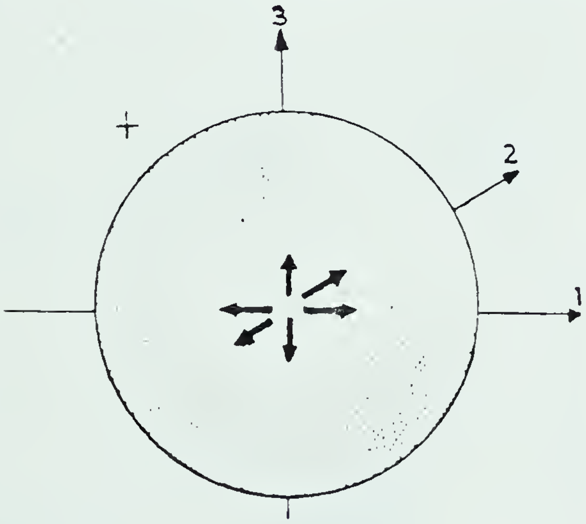

Fig. 2.5a Directivity pattern for P wave from center of dilatation.

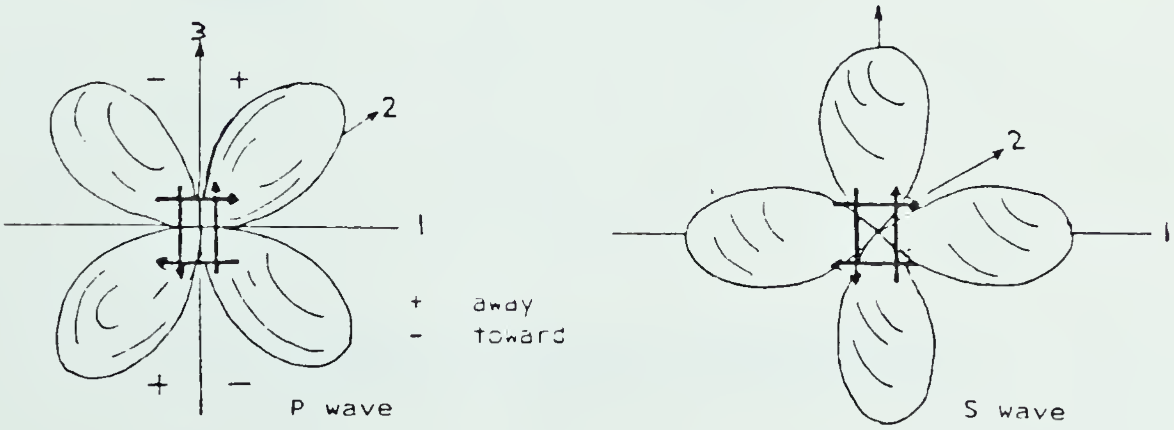

Fig. 2.5b Directivity patterns for double couple.

As various source terms are just combinations of single couple terms, this leads to the ambiguity in the interpretation. The combination of two oppositely signed dipoles at right angles to each other is the same as a double couple (fig. 2.6a). Similarly a suitable combination of a double couple, a center of dilatation and a linear doublet is equivalent to a differently oriented double couple (fig. 2.6b).

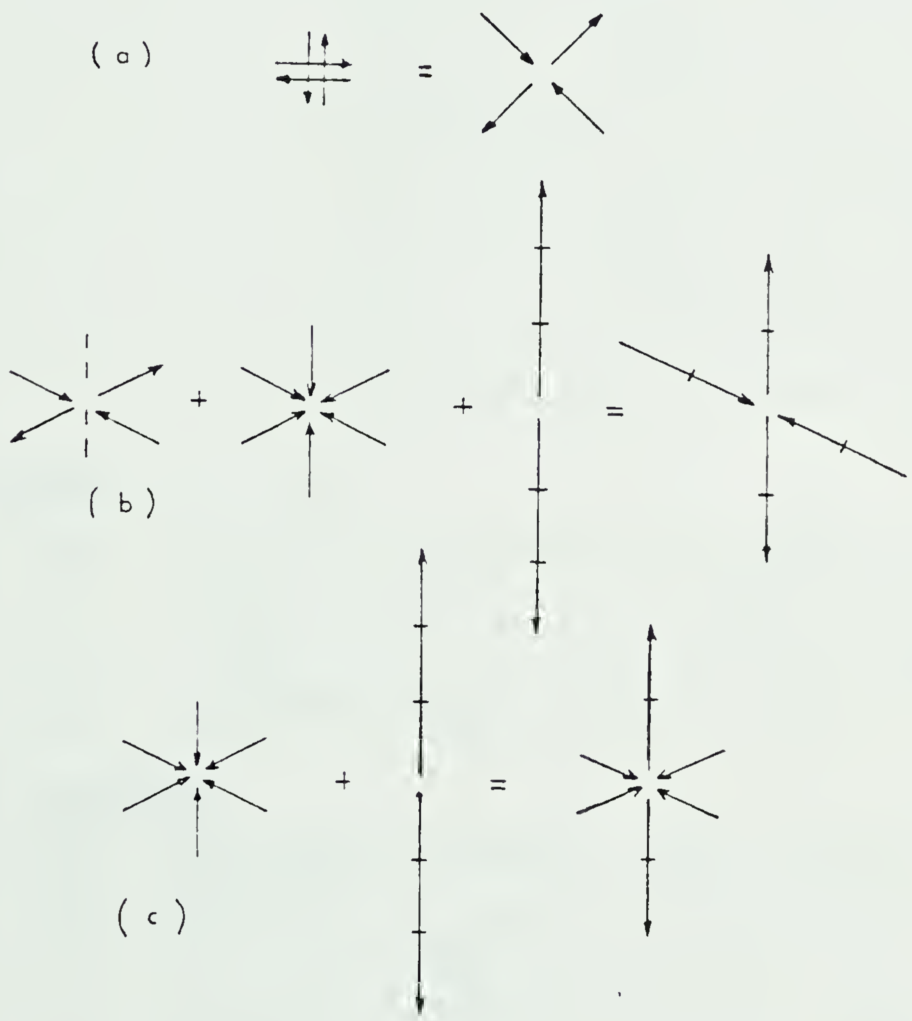

Fig. 2 6 Ambiguity in the source representation

Table 2.1 The source term f for various sources

Source	f
Single force	
1. in the x_1-direction	$\hat{e}_1\,\delta(x_1-x_1')\,\delta(x_2-x_2')\,\delta(x_3-x_3')$
2. in the x_2-direction	$\hat{e}_2\,\delta(x_1-x_1')\,\delta(x_2-x_2')\,\delta(x_3-x_3')$
3. in the x_3-direction	$\hat{e}_3\,\delta(x_1-x_1')\,\delta(x_2-x_2')\,\delta(x_3-x_3')$
Dipole	
1. in the x_1-direction	$-\hat{e}_1\,\frac{\partial}{\partial x_1}\delta(x_1-x_1')\,\delta(x_2-x_2')\,\delta(x_3-x_3')$
2. in the x_2-direction	$-\hat{e}_2\,\delta(x_1-x_1')\,\frac{\partial\delta}{\partial x_2}(x_2-x_2')\,\delta(x_3-x_3')$
3. in the x_3-direction	$-\hat{e}_3\,\delta(x_1-x_1')\,\delta(x_2-x_2')\,\frac{\partial}{\partial x_3}\delta(x_3-x_3')$
Single couple	
1. (12)	$-\hat{e}_1\,\delta(x_1-x_1')\,\frac{\partial\delta}{\partial x_2}(x_2-x_2')\,\delta(x_3-x_3')$
2. (21)	$-\hat{e}_2\,\frac{\partial}{\partial x_1}\delta(x_1-x_1')\,\delta(x_2-x_2')\,\delta(x_3-x_3')$
3. (23)	$-\hat{e}_2\,\delta(x_1-x_1')\,\delta(x_2-x_2')\,\frac{\partial}{\partial x_3}\delta(x_3-x_3')$
4. (32)	$-\hat{e}_3\,\delta(x_1-x_1')\,\frac{\partial}{\partial x_2}(x_2-x_2')\,\delta(x_3-x_3')$
5. (31)	$-\hat{e}_3\,\frac{\partial}{\partial x_1}\delta(x_1-x_1')\,\delta(x_2-x_2')\,\delta(x_3-x_3')$
6. (13)	$-\hat{e}_1\,\delta(x_1-x_1')\,\delta(x_2-x_2')\,\frac{\partial}{\partial x_3}\delta(x_3-x_3')$
Double couple	
1. (23)+(32)	$-\left[\hat{e}_2\,\delta(x_2-x_2')\,\frac{\partial}{\partial x_3}\delta(x_3-x_3')+\hat{e}_3\,\frac{\partial}{\partial x_2}\delta(x_2-x_2')\,\delta(x_3-x_3')\right]\delta(x_1-x_1')$
2. (31)+(13)	$-\left[\hat{e}_3\,\frac{\partial\delta}{\partial x_1}(x_1-x_1')\,\delta(x_3-x_3')+\hat{e}_1\,\delta(x_1-x_1')\,\frac{\partial}{\partial x_3}\delta(x_3-x_3')\right]\delta(x_2-x_2')$
3. (12)+(21)	$-\left[\hat{e}_1\,\delta(x_1-x_1')\,\frac{\partial}{\partial x_2}\delta(x_2-x_2')+\hat{e}_2\,\frac{\partial}{\partial x_1}\delta(x_1-x_1')\,\delta(x_2-x_2')\right]\delta(x_3-x_3')$
Center of rotation	
1. (32)-(23)	$-\left[\hat{e}_3\,\frac{\partial}{\partial x_2}\delta(x_2-x_2')\,\delta(x_3-x_3')-\hat{e}_2\,\delta(x_2-x_2')\,\frac{\partial}{\partial x_3}\delta(x_3-x_3')\right]\delta(x_1-x_1')$
2. (13)-(31)	$-\left[\hat{e}_1\,\delta(x_1-x_1')\,\frac{\partial}{\partial x_3}\delta(x_3-x_3')-\hat{e}_3\,\frac{\partial}{\partial x_1}\delta(x_1-x_1')\,\delta(x_3-x_3')\right]\delta(x_2-x_2')$
3. (21)-(12)	$-\left[\hat{e}_2\,\frac{\partial}{\partial x_1}\delta(x_1-x_1')\,\delta(x_2-x_2')-\hat{e}_1\,\delta(x_1-x_1')\,\frac{\partial\delta}{\partial x_2}(x_2-x_2')\right]\delta(x_3-x_3')$
Center of compression	$-\left[\hat{e}_1\,\frac{\partial}{\partial x_1}\delta(x_1-x_1')\,\delta(x_2-x_2')\,\delta(x_3-x_3')+\hat{e}_2\,\delta(x_1-x_1')\,\frac{\partial}{\partial x_2}\delta(x_2-x_2')\cdot\delta(x_3-x_3')+\hat{e}_3\,\delta(x_1-x_1')\,\delta(x_2-x_2')\,\frac{\partial\delta}{\partial x_3}(x_3-x_3')\right]$

The source term f_i for various point sources are presented in the table 2.1.

The accepted model for the shallow focus earthquake is a double couple. Haskell (1963) has given directivity pattern for a double couple in half space for Rayleigh wave. Burridge et al (1964) and Alterman et al (1970) have studied the effect of burying a double couple directly beneath the free surface of an elastic half space.

For the deep focus earthquakes Knopoff and Randall (1970) proposed a combination of double couple and center of dilatation called compensated linear vector dipole (fig. 2.6c). This combination does not produce volume change, has no net force, no net moment and has five degrees of freedom in spatial orientation.

2.2 Dislocation model:-

In the dislocation representation of the earthquakes the source region is shrunk such that the source boundary S_0 may be regarded as madeup of two sides S_0^+ and S_0^- .The displacement and stress fields on each surfaces are

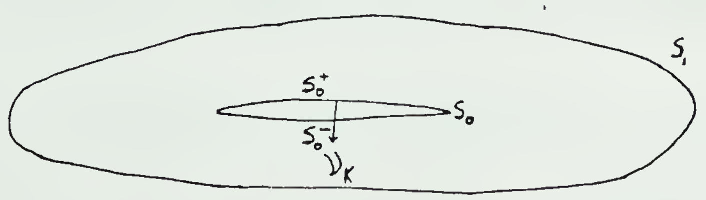

Fig. 2.7 Dislocation surface.

considered to be different. Therefore in the surface term of the equation 2.3, we get a term like $(u_j^+ - u_j^-)$, the superscript + refers to the value at S_o^+ and - at S_o^-, because the normals to the surface are opposing each other.

Defining

$$(u_j^+ - u_j^-) = \Delta u_j$$
$$(u_{p,q}^+ - u_{p,q}^-) = \Delta u_{p,q} \qquad 2.21$$

which may be regarded as a jump in the displacement and stress fields on S_o, and putting it into the eq. 2.3, we get

$$u_i(\vec{x},t) = \int_{-\infty}^{+\infty} dt' \int_V G_{ij}(\vec{x},t;\vec{x}',t') f_j(\vec{x}',t') d^3\vec{x}' + \int_{-\infty}^{+\infty} dt' \int_{S_o} \{\Delta u_j(\vec{\xi},t') C_{jkpq} \qquad 2.22$$
$$G_{ip,q}(\vec{x},t;\vec{\xi},t') - G_{ij}(\vec{x},t;\vec{\xi},t') C_{jkpq} \Delta u_{p,q}(\vec{\xi},t')\} \nu_k d^2\vec{\xi}$$

In the above equation for the surface integration a new variable $\vec{\xi}$ is used to distinguish as it runs only on the surface S_o, and hereafter S_o will be called Σ.

Introducing the Radon transformed Green's function

$$G_{ij}(\vec{x},t;\vec{\xi},t') = \int_V \delta(\vec{x}'-\vec{\xi}) G_{ij}(\vec{x},t;\vec{x}',t') d^3\vec{x}'$$
$$G_{ip,q}(\vec{x},t;\vec{\xi},t') = -\int_V G_{ip}(\vec{x},t;\vec{x}',t') \frac{\partial \delta(\vec{x}'-\vec{\xi})}{\partial x_q} d^3\vec{x}' \qquad 2.23$$

plugging it into the equation 2.22, we get

$$u_i(\vec{x},t) = \int_{-\infty}^{+\infty} dt' \int_V G_{ip}(\vec{x},t;\vec{x}',t') \Big(f_p(\vec{x}',t') - \int_\Sigma \{\Delta u_j(\vec{\xi},t) C_{jkpq} \delta_q(\vec{x}'-\vec{\xi}) \qquad 2.24$$
$$+ \Delta u_{p,q}(\vec{\xi},t') C_{pkjq} \delta(\vec{x}'-\vec{\xi})\} \nu_k d^2\vec{\xi} \Big) d^3\vec{x}'$$

The solution with homogeneous boundary conditions on S_1 without any jump conditions on Σ is simply space-time convolution of the Green's function with body force term. Since in the above equation, the surface integral within middle bracket is involved in the same way as f_p ; it may be concluded that the effect of a jump across Σ , has the same effect as introducing an extra body force term $e_p(\vec{x},t)$, given by

$$e_p(\vec{x},t) = -\iint_{\Sigma}\{\Delta u_j(\vec{\xi},t)C_{jkpq}\delta_q(\vec{x}-\vec{\xi}) + \Delta u_{j,q}(\vec{\xi},t)\, C_{pkjq}\,\delta(\vec{x}-\vec{\xi})\}\,\nu_k\, d^2\vec{\xi} \qquad 2.25$$

into an unfaulted medium. Therefore the Green's function for an infinite domain is valid here too.

Using

$$\Delta T_p = \nu_k\, C_{pkjq}\, \Delta u_{j,q}$$

we get a relation expressing the equivalence of the body force and the discontinuity of displacement and stress as

$$e_p(\vec{x},t) = -\int_{\Sigma}\{\Delta u_j\, \nu_k\, C_{jkpq}\,\delta_q(\vec{x}-\vec{\xi}) + \Delta T_p\,\delta(\vec{x}-\vec{\xi})\}\, d^2\vec{\xi}\,. \qquad 2.26$$

Putting 2.26 into 2.24 and performing the time integration we get the displacement field

$$u_i(\vec{x},t) = \int_V \{G_{ip}[f_p] - G_{ip}[e_p]\}\, d^3\vec{x}' \qquad 2.27$$

where $G_{ip}[\phi]$ is defined as in the equation 2.5 .

As f_p is a body force in the source free region, so neglecting it we get the displacement field due to the dislocation source

$$u_i(\vec{x},t) = -\int_V G_{ip}[e_p]\, d^3\vec{x}'$$

Thus knowing the dislocation surface or source boundary Σ and the jump discontinuity across it, the body force term can be calculated, which, on integration with the full space Green's function, will give the displacement field.

In an earthquake on the dislocation surface, the stress discontinuity does not exist because along the dislocation direction the component of stress vanishes and is continuous in all other directions. Therefore, the term ΔT_i may be dropped in the equation 2.26 and $\Delta u_j(\vec{\xi},t)$ will be the displacement field jump across Σ . The expression for the far field P wave can be obtained using the Green's function for that part only as

$$u_i^P(\vec{x},t) = -(4\pi\rho)^{-1} \frac{\partial}{\partial x_q} \int_\Sigma C_{jkpq}\, \gamma_i \gamma_p (v_p^2 r)^{-1} \Delta u_j(\vec{\xi}, t - r/v_p)\, \nu_k\, d^2\vec{\xi} \qquad 2.29$$

$$\approx -(4\pi\rho)^{-1} \int_\Sigma C_{jkpq}\, \gamma_i \gamma_p (v_p^2 r)^{-1} \Delta u_j(\vec{\xi}, t - r/v_p) \left(-\frac{1}{v_p}\frac{\partial r}{\partial x_q}\right) \nu_k\, d^2\vec{\xi} \qquad 2.30$$

In the equation 2.30 another three terms attenuating as r^{-2} are dropped. Further, in the far field $r = |\vec{x} - \vec{\xi}|$ is much larger than the dimension of Σ, so all terms involving r in the equation 2.30 may be regarded as nearly constant and can be pulled outside the integration, except the time delay term in $\Delta \dot{u}_j$ which will vary strongly for small changes of r. Assuming the dislocation is linearly polarized in the direction n_j, ie, $\Delta u_j = n_j \, \Delta u(\vec{\xi}, t)$ we have

$$u_i^P(\vec{x},t) \approx (4\pi\rho v_P^3 r)^{-1} \left(C_{jkpq} \gamma_i \gamma_p \gamma_q \nu_k n_j \right) \int_\Sigma \Delta \dot{u}(\vec{\xi}, t - r/v_P) \, d^2\vec{\xi} \quad 2.31$$

Similarly the far field S wave term is:

$$u_i^S(\vec{x},t) \approx -(4\pi\rho v_S^3 r)^{-1} \left(C_{jkpq} (\gamma_i \gamma_p - \delta_{ip}) \gamma_q \nu_k n_j \right) \int_\Sigma \Delta \dot{u}(\vec{\xi}, t - r/v_S) \, d^2\vec{\xi} \quad 2.32$$

It is evident that the P wave is only longitudinal while the S wave is only transverse. The first part in the above equations 2.31 and 2.32 suggests that both P and S waves attenuate as r^{-1}. The second part involving the direction cosine of the point of observation, the dislocation surface orientation(ν_k) and the direction of the dislocation (n_j) gives the directivity pattern. The third part involving integration of the discontinuity over the dislocation surface gives the wave form and has information about the dislocation surface dimension and the amount of dislocation. In observational seismology, an idea about the

orientation of the dislocation surface and dislocation direction is obtained from the directivity pattern. By analysing the wave form (actually spectra), an estimate about fault plane dimension and the amount of dislocation is obtained.

Let us examine the directivity pattern for a slip dislocation.

Here $K=j$, so we have only two non vanishing terms

$p=K$, $q=j$, and $p=j$, $q=K$

and $C_{jKKj} = C_{jKjK} = \mu$

For the P wave the directivity pattern yields $2\mu\gamma_i\gamma_j\gamma_K$

and for the S wave $\mu\gamma_K(\gamma_i\gamma_j - \delta_{ij}) + \mu\gamma_j(\gamma_i\gamma_K - \delta_{iK})$

These terms are same as the radiation pattern for far field P and S terms, respectively, for a double couple. Since we do not have a priori knowledge of dislocation surface, it may, to a first appoximation be shrunk to a point, ie,

$$\Delta u \propto \delta(\xi_1)\,\delta(\xi_2)\,F(t)$$

so

$$\int \Delta\dot{u}\, d^2\xi \longrightarrow \dot{F}(t - r/v_p)$$

which is same as the wave term for double couple. Thus in

all respects a point slip dislocation is equivalent to a double couple in an unfaulted medium.

For any arbitrary dislocation surface, one may create a source such as a distribution of point sources over a finite region acting simultaneously. Alternatively one can have a point source tracing out a moving pattern over a finite volume of material. The first case can be thought of as the infinite velocity limit of the second case. In either example, one has to formulate the point source problem from the point dislocation (surface) model, and then sum up the effect of the distribution by integrating over space.

Ben-Menahem (1961) studied the radiation pattern of surface waves and later (Ben-Menahem, 1962) for body waves. For a simple model of fault by considering a moving point source, he has shown that the finiteness of the seismic source plays an important role in the radiation pattern whenever the dominant wavelength of the source spectra is of the order of the dimension of the fault or when the time of rupture is of the order of the period. Here the spectrum is modulated by $\sin X/X$ type of function,

$$A(\omega, \theta) \simeq \frac{\sin\left[\frac{\omega b}{2V_\omega}\left(\frac{V_\omega}{V_r} - \cos\theta\right)\right]}{\left[\frac{\omega b}{2V_\omega}\left(\frac{V_\omega}{V_r} - \cos\theta\right)\right]}$$

θ =Azimuthal angle of point of observation from source

b =Source length

V_w =Velocity of propagation of particular phase

V_r =velocity of propagation of moving source or rupture velocity

It was also demonstrated that effective fault length and rupture velocity can be recovered by taking the ratio of the displacement of the same spectral component, at two stations which are located symmetrically with respect to the source. This ratio is

$$\vec{D} = \frac{\left[\frac{V_w}{V_r} + \cos\theta\right]}{\left[\frac{V_w}{V_r} - \cos\theta\right]} \frac{\sin\left[\frac{wb}{2V_w}\left(\frac{V_w}{V_r} - \cos\theta\right)\right]}{\sin\left[\frac{wb}{2V_w}\left(\frac{V_w}{V_r} + \cos\theta\right)\right]} e^{\frac{i\,2\pi\, b w \cos\theta}{V_r}}$$

the vector $\vec{D}$ is called vector directivity; its magnitude and phase are obtained for all spectral frequencies and by comparing it with theoretical results, the fault parameters b and V_r are deduced.

Hirasawa and Stauder (1965) and Savage (1965) considered that the time after which the wave arrives at the observation point is short compared to the time for rupture to traverse the source region. Thus they ignored the effect of cessation of motion (stopping phase). Savage explicitly gave the following modulating function in this case

$$F_1(\theta) = \frac{V_r}{\left(1 - \frac{V_r}{V_w}\cos\theta\right)}$$

for unilateral faults and

$$F_2(\theta) = \frac{2V_r}{\{1-(V_r/V_w)^2\cos^2\theta\}}$$

for bilateral faults.

This yields that the nodal planes of the original directivity pattern are unchanged; a point made by Hirasawa and Strauder.

Savage has also shown that the resulting response is roughly rectangular and has time duration proportional to $b/F_1(\theta)$. Therefore the product of amplitude (which depends upon $F_1(\theta)$ and the time duration does not depend strongly upon the direction of dislocation propagation since the factor $F_1(\theta)$ is cancelled. This is essentially same as Ben-Menahem result for small b or large T.

The analysis for arbitrary source can be systematized by expanding the Green's function in vector spherical harmonics. Carrying out the integration 2.3 leaves the displacement represented as a summation over vector spherical harmonics, a multipole expansion. One then identifies the individual terms with simple forces, couples, double couples, center of dilatation, etc. (Archambeau (1968), Ben-Menahem and Singh (1972), Randall (1972)). An extensive study on unified approach to the representation of seismic sources has been done by Singh et al (1973).

A more sophisticated approach is developed by Backus and Mulcay (1976a,76b), and Backus (1977a,77b) who presented a thorough analysis of the sources in tensor formulation. They describe a number of different ways of representing an arbitrary indigenous seismic source, introduce the concept of stress glut, discuss the uniqueness of the various source descriptions, and outline a method of expanding a source representation in a series of polynomial moments.

A more realistic model for an arbitrary source will be to assume that the point dislocation propagates itself instead of the point source equivalent of point dislocation. Here a rupture criterion for the propagation of a point dislocation can be incorporated to take into account rock strength, friction etc. This approach is known as crack propagation. In the past few years extensive work has been done on this aspect of dislocation model. In chapter IV we will systematically outline the development of this approach.

3. SEISMIC SPECTRUM

We know that a waveform is given (say for P wave) by

$$\int_{\Sigma} \Delta \dot{u} (\vec{\xi}, t - r/v_p) d^2\vec{\xi} \tag{3.1}$$

Therefore the observed waves, ie, seismograms, can tell us about the fault dimension Σ and dislocation Δu.

A practical approach to this inverse problem is to describe Σ and Δu with a small number of parameters. We consider the simplest of such models: a unidirectional propagating dislocation.

We assume that Σ is rectangular with the longer side as fault length (L) and shorter side as fault width (W). We also assume that the dislocation starts at $\vec{\xi} = 0$ and propagates along the fault length with rupture velocity v, and that the dislocation has identical form at any $\vec{\xi}$. We call this time function 'source time function' and write it $D(t)$.

By the above parameterization $\Delta u(\vec{\xi}, t)$ can be written as

$$\Delta u(\vec{\xi}, t) = D(t - \xi_1 / v) \tag{3.2}$$

where the ξ_1 axis is taken along the fault length L.

With above, the expression 3.1 becomes

$$\int_{\Sigma} \Delta \dot{u}(\vec{\xi}, t - r/v_p)\, d^2\vec{\xi} = W \int_0^L \dot{D}(t - r/v_p - \xi_1/v)\, d\xi_1 \qquad 3.3$$

This gives the wave form for far-field P waves. Since we are concerned about the far-field, we can put

$$r = r_0 - \xi_1 \cos\theta$$

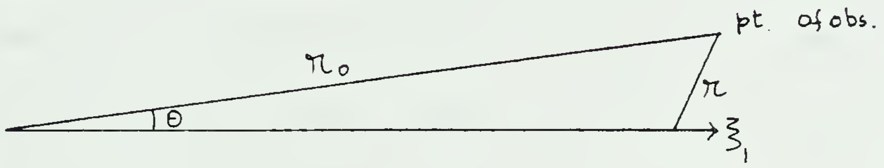

Fig. 3.1

Then the equation 3.3 may be written as

$$\int_{\Sigma} \Delta \dot{u}(\vec{\xi}, t - r/v_p)\, d^2\vec{\xi} = W \int_0^L \dot{D}(t - r_0/v_p - \xi_1(1/v - \cos\theta/v_p))\, d\xi_1$$

$$= \frac{WL}{T_L} \int_0^{T_L} \dot{D}(t - r_0/v_p - t')\, dt' \qquad 3.4$$

where

$$t' = \xi_1 (1/v - \cos\theta/v_p)$$

$$T_L = L(1/v - \cos\theta/v_p)$$

The above equation shows that the observed wave form is a moving average of $\dot{D}$ over the time interval T_L .

From the equations 2.31 and 3.4 the far-field P waves can be expressed as

$$\vec{F}(\vec{x},t) = \gamma_i \cdot U_i^P(\vec{x},t) = (4\pi\rho v_p^3 r)^{-1}(C_{jkpq}\gamma_p\gamma_q\nu_k n_j)\frac{WL}{T_L}\int_0^{T_L}\dot{D}(t-r_0/v_p-t')dt' \qquad 3.5$$

In order to determine the source parameters by comparing the above theoretical wave form with the observed, it is convenient to work in the frequency domain. We define 'the seismic spectrum' as the Fourier transform of the ground displacement:

$$F(\vec{x},\omega) = (4\pi\rho v_p^3 r)^{-1}(C_{jkpq}\gamma_p\gamma_q\nu_k n_j)\frac{WL}{T_L}\int_{-\infty}^{+\infty}e^{-i\omega t}dt\int_0^{T_L}\dot{D}(t-r/v_p-t')dt'$$

Defining

$$V(\omega) = \int_{-\infty}^{+\infty}\dot{D}(t)\,e^{-i\omega t}dt \qquad 3.6$$

we have ,

$$F(\vec{x},\omega) = (4\pi\rho v_p^3 r)^{-1}(C_{jkpq}\gamma_p\gamma_q\nu_k n_j)\frac{WL}{T_L}e^{-i\omega r_0/v_p}\,V(\omega)\,\frac{\sin\frac{\omega T_L}{2}}{\omega/2}\,e^{-i\omega T_L/2}$$

Here the amplitude spectrum is

$$|F(\vec{x},\omega)| = (4\pi\rho v_p^3 r)^{-1}(C_{jkpq}\gamma_p\gamma_q\nu_k n_j)\,WL\,V(\omega)\,\frac{\sin X}{X} \qquad 3.7$$

where

$$X = \frac{WT_L}{2} = \frac{WL}{2}\left(\frac{1}{v} - \frac{\cos\theta}{v_p}\right)$$

and phase spectrum

$$\phi(\omega) = \frac{\omega}{v_p} r + \frac{\omega}{2} T_L + \phi_v(\omega)$$

where $\phi_v(\omega)$ is the phase spectrum for dislocation velocity $\underset{\sim}{V}(\omega)$

$$\underset{\sim}{V}(\omega) = |\underset{\sim}{V}(\omega)|\, e^{-i\phi_v(\omega)}$$

The equation 3.7 describes the charecteristics of amplitude spectra of P waves. Similar expression may be obtained for S waves. Let us examine the spectrum starting from very low frequency. For small ω, X is small so $\sin X/X$ is nearly unity. Also $|\underset{\sim}{V}(\omega)|$, for small ω, is almost a constant, equal to permanent off-set. From equation 3.6 for zero frequency

$$\underset{\sim}{V}(0) = \int_{-\infty}^{+\infty} \dot{D}(t)\,dt = D(+\infty) - D(-\infty)$$

which is equal to permanent off-set ΔD across the fault plane. Thus from the equation 3.7, we have

$$\underset{\sim}{F}(\vec{x},0) = (4\pi\rho v_p^3 r)^{-1} (C_{jkpq}\gamma_p \gamma_q \nu_k n_j)\, WL\Delta D$$

Since the maximum value of $C_{jkpq}\gamma_p\gamma_q\nu_k n_j$ is μ for slip dislocation in an isotropic body then

$$4\pi\rho v_p^3 r\, \underset{\sim}{F}(\vec{x},0) = \mu WL\Delta D$$

The quantity on the right hand side is called seismic moment, can be readily obtained from the zero frequency amplitude. It is also evident that the spectrum at low frequencies will be flat.

For higher frequency, the factor $\sin X/X$ in the equation 3.7 produces a θ dependent spectrum. The envelope of $\sin X/X$ is proportional to ω^{-1}. This smoothing effect is weakest in the direction of rupture propagation ($\theta=0$) and strongest in the opposite direction ($\theta=\pi$). As a result more high frequency waves will be observed in the propagation direction.

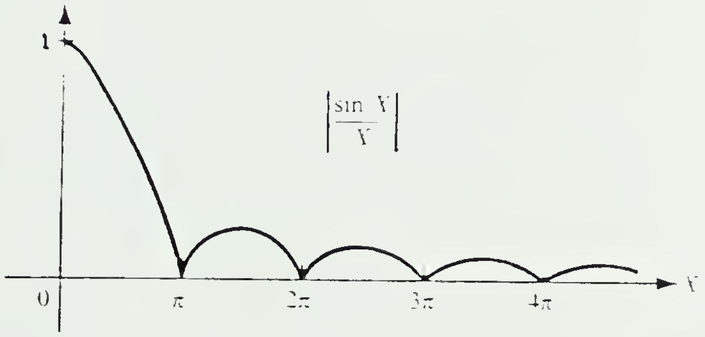

Fig. 3.2

The $\underset{\sim}{V}(\omega)$ part will also modulate the spectrum according to the choice of source time function $D(t)$. The simplest form of the function may be a step function. In that case $\dot{D}(t)$ is proportional to $\delta(t)$ and

$$\underset{\sim}{V}(\omega) = \int \dot{D}(t)\, e^{-i\omega t}\, dt = \text{Constant}$$

So the step function is physically impossible for

spontaneous rupture, because the far-field wave will have infinite seismic energy. Therefore 'rise time', a finite duration over which $D(t)$ rises(Ben-Menahem and Toksoz (1963), Haskell (1964)), is introduced. Usually they are assumed to be ramp or exponential functions.

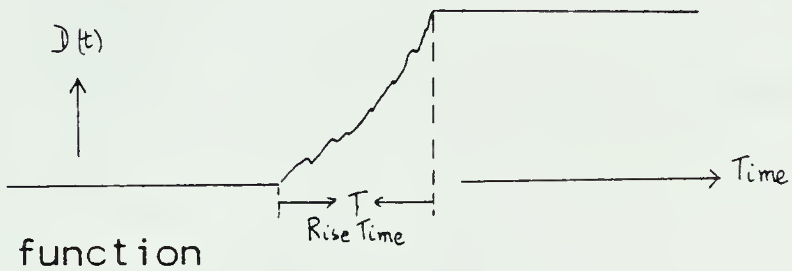

For a step function

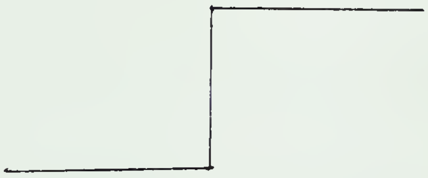

$$|V(\omega)| = \text{Constant}$$

For a ramp function

$$|V(\omega)| = \frac{e^{-i\omega T} - 1}{\omega^2 T}$$

For a exponential function

$\left(1 - e^{-t/T}\right)$

$$|V(\omega)| = \frac{1}{i\omega(1+i\omega T)}$$

In any case, the finite rise time introduces an additional factor proportional to ω^{-1} at high frequencies. Thus, we have a general feature of the seismic spectrum as

shown in the fig. 3.3.

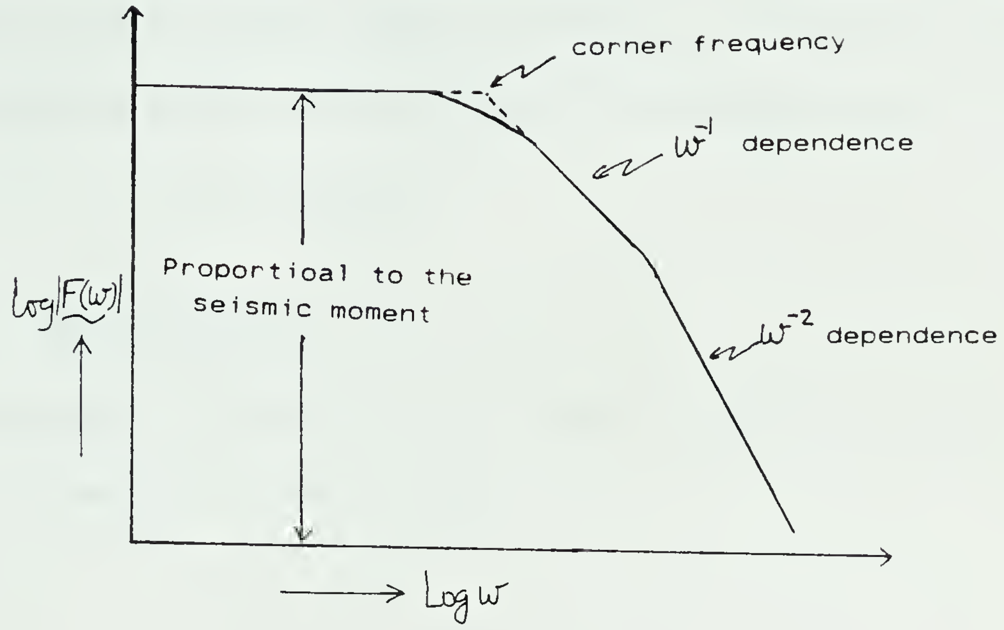

Fig. 3.3 Seismic spectrum.

There are other dislocation models in which the rupture propagation is two-dimensional (Savage, 1966). In such cases, the smoothing effect at higher frequencies is proportional to ω^{-2} instead of ω^{-1} of the uni-directional propagating dislocation. This gives ω^{-3} dependence at the highest frequencies.

Apart from the low frequencies constant level and higher frequencies proportionality to negative powers of frequency there is another feature in the spectrum which is defined by the intersection of the low and high frequency trends. This is called 'corner frecquency' and is related to the length of the fault (Brune, 1970).

For an ensemble of earthquakes with a wide range of magnitude we can construct a scaling law of seismic spectrum. For example , if we assume that a large earthquake and a small one are physically similar, we find out that the source parameters should satisfy following conditions,

$$L \propto W \propto \Delta D \propto T$$

and υ =constant.

Then, the seismic spectrum will take following shape for the case of ω^{-2} model (Aki, 1967).

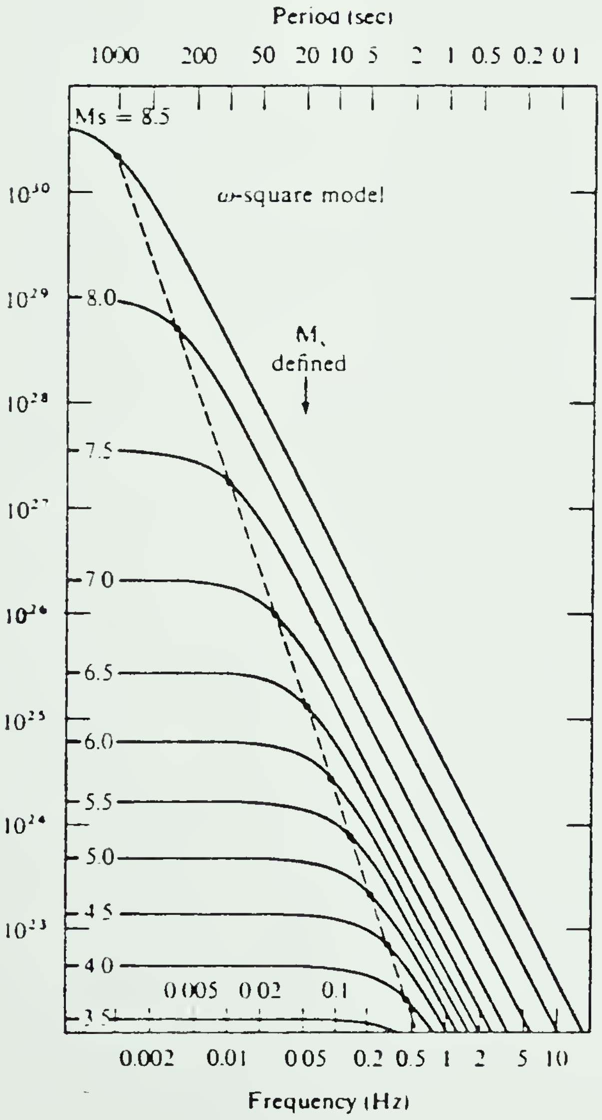

Fig. 3.4 Seismic spectra for an ensemble of earthquakes (Aki, 1967).
The broken line is locus of corner frequency, proportional to ω^{-3}.

From the similarity assumption, the corner frequency inversely proportional to the source length and seismic moment is proportional to the cube of source length. Therfore, the seismic moment is inversely proprotional to the cube of the corner frequency. The results are shown in the fig. 3.4.

Simple models discussed above are extensively used for the source parameters determination. For predicting seismic effects of dangerous earthquakes or distinguishing nuclear tests more complicated model should be considered.

4. DYNAMICS OF THE SOURCES

In order to find the displacement field from a dislocation model of the earthquake an intregation over the dislocation surface, $\vec{\Sigma}(\vec{x},t)$, of the displacement field discontinuity, $\Delta u_i(\vec{x},t)$, has to be carried out. As a first order of appoximation the inhomogeneities present in the earth's crust seem enough to cause variation in the rock strength and friction and to create the local stress build-ups. A stress concentration, sufficient to overcome the resistance of the rock to fracture, will start the crack and when stress diminishes or the resistance increases the crack will stop. Therefore, it may be visualized that depending upon conditions of stress, rock strength and friction a rupture front nucleates from a point, then spreads over a region with some finite velocity and finally ceases to run, resulting in some distribution of the displacement field discontinuity over the dislocation surface formed due to the crack. Thus the dislocation surface is a function of space and time and has to be determined along with the discontinuity of the displacement field over it from the condition of initial stresses, rock strength and friction. Mathematically the problem may be formulated as follows.

Let the medium with elastic moduli C_{ijpq} and density ρ be held by a constant stress σ^{o}_{ij}. At time t=0, a crack nucleates at the origin and spreads, so at time t>0 it covers the surface $\vec{\Sigma}(\vec{x},t)$. Let $u_i(\vec{x},t)$ be the displacement field measured relative to the state of strain prevailing for t=0,

We have,

$$\sigma_{ij} = C_{ijpq}\, u_{p,q}$$

and the total stress in the medium is then

$$\sigma^{T}_{ij} = \sigma^{o}_{ij} + \sigma_{ij}$$

Due to the crack there is relative movement of the parts of the medium adjacent to the different sides of $\vec{\Sigma}$; if $\pm$ denotes the limiting value of u_i on two sides of $\vec{\Sigma}$,

$$u_i^{+} - u_i^{-} = \Delta u_i$$

If n_i denotes the positive normal, then for tensile cracks

$$\Delta u_i \cdot n_i > 0 \quad ; \quad \Delta u_i \times n_i = 0$$

And for sliding crack

$$\Delta u_i \cdot n_i = 0 \quad ; \quad \Delta u_i \times n_i > 0$$

The position of area of crack at each moment is determined by a contour surrounding the edge of the crack; let ν_i be the unit tangent to it, then the velocity of propagation of edge v_i will be normal to n_i as well as ν_i.

$$v_i \cdot n_i = 0 \qquad ; \qquad v_i \cdot \nu_i = 0$$

The propagation will be determined by some physical desirable condition of energy dissipation in the growth of the crack, which may be deduced by considering the surface free energy or cohesion or some other criterion. This is known as crack propagation criterion and will be discussed in detail in the next section.

Moreover, in accordance with the causality condition the crack propagation velocity should not be greater than the P wave velocity,

$$|\vec{v}| \leq v_p$$

Also outside the crack the displacement discontinuity should vanish,

$$\Delta u_i = 0 \qquad , \quad \not\subset \vec{\Sigma} \tag{4.1}$$

The surface of the rupture should be free from traction; this gives the following condition

$$\sigma_{ij}^T \cdot n_i = 0 \qquad \subset \vec{\Sigma} \tag{4.2}$$

Therefore the problem is specified by the equation of motion

$$\rho \ddot{u}_i - (C_{ijpq} u_{p,q})_{,j} = 0 \qquad 4.3$$

subject to the boundary conditions 4.1 and 4.2 together with the rupture criterion and the initial conditions

$$u_i = \dot{u}_i = 0 \qquad t \leq 0 \qquad 4.4$$

In the above formulation, to solve the equation of motion, prior knowledge of $\vec{\Sigma}(\vec{x},t)$ and the normal n_i to $\vec{\Sigma}(\vec{x},t)$ are required. For the sake of simplicity it is assumed that the crack developes along some preferred plane so n_i is known. Also assuming that the growth of the crack takes place in some specific mode and with knowledge of the propagation velocity $\vec{v}$, the dislocation surface $\vec{\Sigma}(\vec{x},t)$ may be defined.

In general the surface $\vec{\Sigma}(\vec{x},t)$ may be irregularly shaped but the restriction to the crack surface imposed above makes the solution for the displacement field not so appropriate for the near field region, where the details of the surface $\vec{\Sigma}(\vec{x},t)$ may have profound influence on the radiation field. However, for the far field region these minute details which have been excluded donot have any influence on the displacement field.

There are three basic modes of the crack growth (Bilbly and Eshelby, 1968), in each the crack occupies the plane $X_3=0$ and $-\upsilon t < x_1 < \upsilon t$ & $-\infty < x_2 < \infty$ (fig. 4.1).

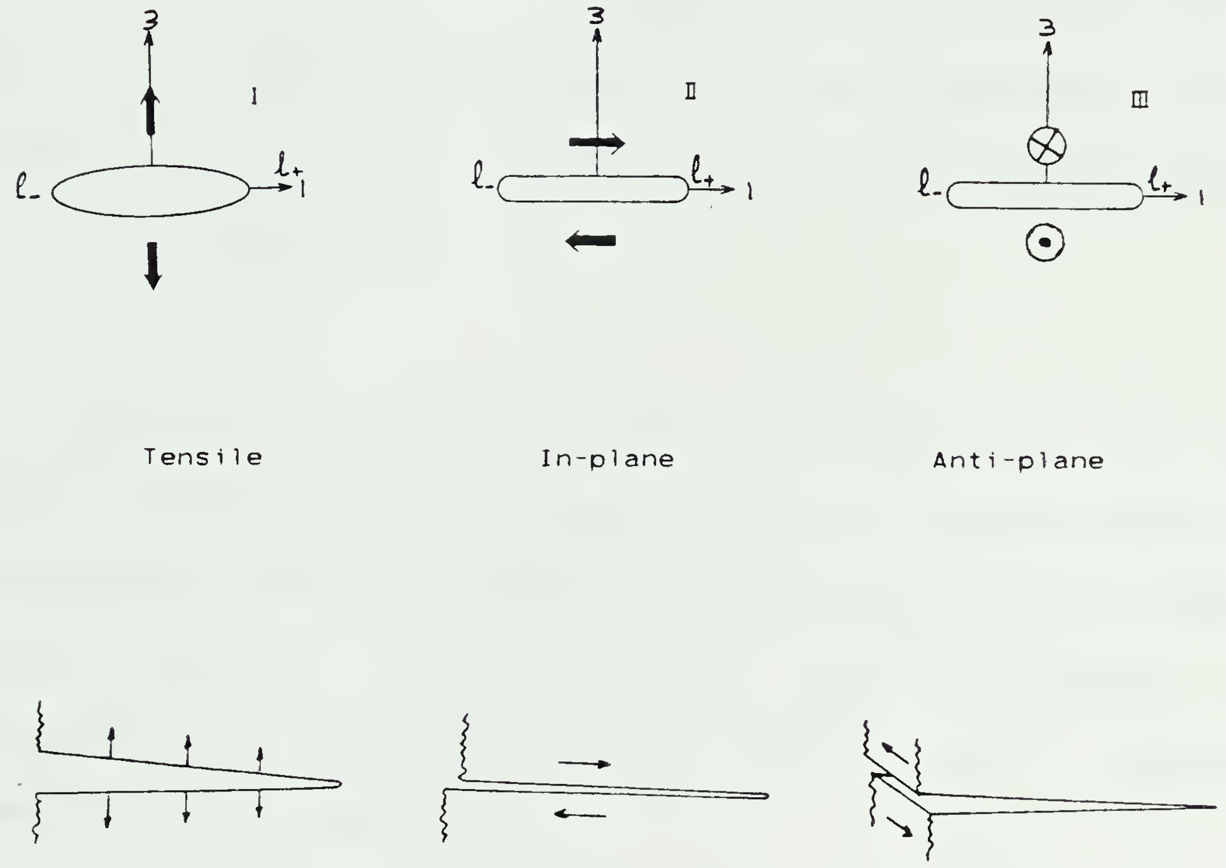

Fig 4.1 Three basic modes of crack propagation.

I Tension mode

The state of tension mode of crack opening is defined by $\Delta U_3 = f(x_1)$ on the crack plane, ie, $X_3=0$ together with only one non vanishing component of initial stress namely σ^0_{33} .

II In-plane mode

The faces of the crack slide past one another as indicated by the arrow, the crack opening is

defined by $\Delta u_i = f_1(x_1)$ on $x_3=0$ and the only non zero initial stress is σ^0_{13} .

III Anti-plane mode

The faces of the crack move in and out of the figure,as indicated by the arrow head and tail, here $\Delta u_2 = f_2(x_1)$ on $x_3=0$ with the only non vanishing initial stress σ^0_{23} .

Tension crack opening mode is appropriate for regions under tension stress, such as ridges, but at a depth below few hundred meters lithospheric pressure would keep the faces together, so a suitable mode of rupture may be in-plane or anti-plane shear crack or in general a combination of both.

The problem assumes that the growth of crack starts at $t=0$. Strictly speaking the presence of a small crack at the origin at initial time is assumed, although the dimension of that small opening is not taken into the account in mathematical formulation.

Further, invoking symmetry and anti symmetry of stresses and displacement fields about the plane $x_3=0$, the full space problem may be reduced to a b.v.p. for half space. Thus the solution has to be found in only one region and using symmetry arguments the solution in the other region can also be found.

Most of the work done so far in seismic source dynamics consists of solving the problem formulated above for different growth modes with different crack propagation criteria .

4.1 Crack propagation criteria:-

To describe the process of rupture as a spontaneous phenomenon, one has to specify the change in dimension of the crack in addition to the boundary conditions at the surface of the crack. Griffith (1920) described this change in dimension by considering global energy balance in the material. Barenblatt (1962) considered a yielding mechanism at the crack tip and developed another fracture criterion.

Griffith energy balance model:-

Griffith (1920) formulated crack propagation criteria in terms of energy balance of the whole material surrounding the crack. There are always weak zones inside a material and under the applied load, if the rate of release of mechanical energy (applied load work done W_L plus strain energy U_E stored in the medium) exceeds a certain minimum value, growth of these zones takes place resulting in the development of the cracks whereby new surfaces having some

surface energy U_s are created. Therefore, the total energy of the system is,

$$U = (-W_L + U_E) + U_s \qquad 4.5$$

The condition for a crack to grow, therefore is that the decrease in mechanical energy should be just greater than the increase in surface energy. Thus, under equilibrium condition

$$\frac{dU}{da} = 0 \qquad 4.6$$

where a is a measure of crack length.

Clearly, the crack would extend or close up reversibly for small displacements from the equilibrium length, according to whether the left-hand side of 4.6 is negative or positive.

The theoretical calculation as well as observed facts suggest that there is stress concentration near the tip of the crack and the growth of crack occurs when it exceeds a certain critical value. Irwin (1958) introduced the concept of stress intensity factor (the stress at the tip of an infinitely sharp crack due to the remote stress), K, and extended the Griffith concept to account for the behaviour of real materials by considering a dissipative component in the potential energy term to account for nonlinearity at the crack tip.

One defines the crack extension force (the mechanical strain energy release rate per unit width of the crack front) as (Lawn and Wilshaw, 1975, p.50),

$$G = -\frac{d(-W_L+U_E)}{d\,a}$$

which is related to K through elastic constants .

One also defines the fracture surface energy, Γ ,as (Lawn and Wilshaw, 1975, p.79),

$$2\Gamma = \frac{dU_s}{da}$$

At Griffith equilibrium, 'the so called Irwin and Orwan generalization of the Griffith criterion' (Lawn and Wilshaw, 1975, p. 79) is

$$G_c = 2\Gamma$$

where the subscript c refers to the equilibrium value.

So fracture will extend if $G > 2\Gamma$

If there is no dissipative component in the work of creating new fracture surface,

$$\Gamma = \gamma$$

where γ is the reversible surface energy of an ideal brittle solid.

As the crack starts to propagate, material near the sides of the crack is displaced. The rate at which this

material can move limits the velocity of the crack propagation. Following the Mott (1948) procedure, a kinetic energy term, U_K, is added to the expression for the total energy and invoking the equation 4.6 the fracture criterion is:

$$G - \frac{dU_K}{da} > 2\Gamma \qquad 4.7$$

<u>Cohesive zone model:-</u>

Barenblatt (1962) developed the cohesive zone model by considering crack propagation on the atomic level, where it may be visualized as breaking of the bonds between the atoms at the crack tip. The force holding atoms together is plotted against inter-atomic separation (fig. 4.2).

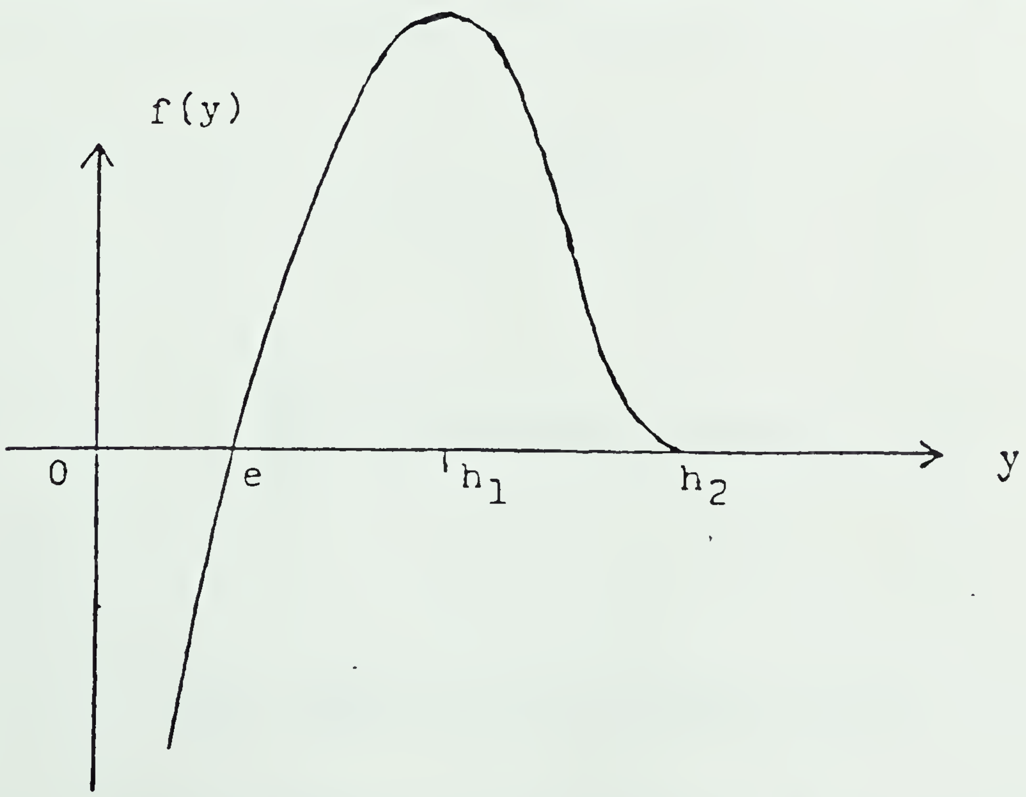

Fig. 4.2 Cohesive force between atoms as a function of their separation distance

At equilibrium separation e the force is zero; with the increase of the separation it grows and reaches a maximum for the separation h_1 and after that it diminishes rapidly with further increase and beyond h_2 it may be regarded as zero. Therefore, it may be assumed that beyond h_1 a weakening of bonds starts and at h_2 it is completely broken. Thus at the tip of the crack the inter-atomic separation will be of the order of h_1 and cohesive force will be maximum there, and trailing behind will be a zone with steadily increasing separation, which will run into the completely fractured region with zero cohesive force beyond the point where separation is of the order of h_2 (fig. 4.3).

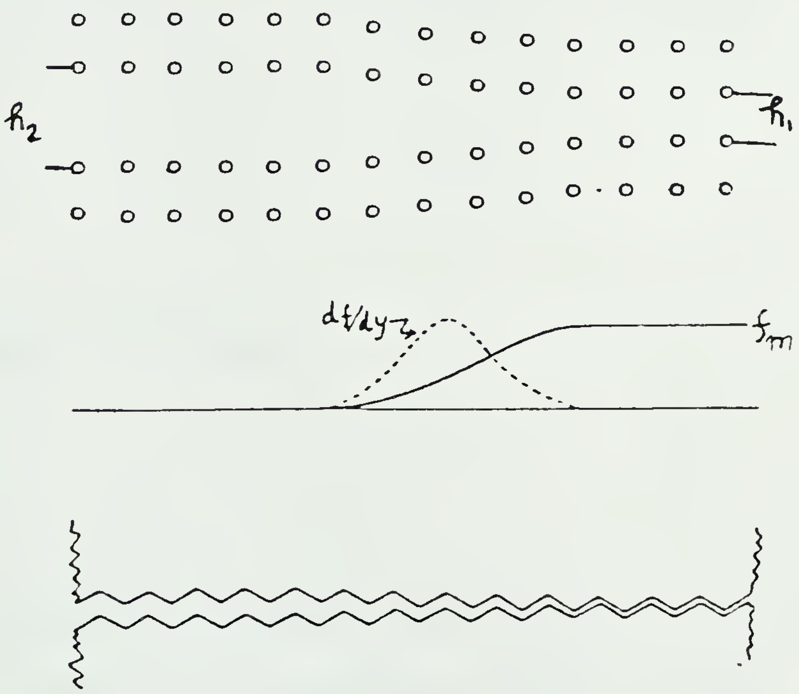

Fig. 4.3 Atomic view of the fracture process.

Clearly the gradient of the cohesive force, ie, stress field

will have a hump which is of the order of a few atomic distance over the transition zone. The amount of work to produce unit area of crack between originally unseparated planes of atoms equal to

$$\sigma^c = n \int_{h_1}^{h_2} f(y)\, dy$$

must be done against the cohesive force; where n is the number of bonds per unit area. With this, the expression for the stress intensity factor (Bilbly and Eshelby, 1968)is:

$$K = \sqrt{\frac{2}{\pi}} \int_{-d}^{0} \sigma^c(x_1)\,(-x_1)^{-1/2}\, dx_1$$

where d is the dimension of region over which the cohesive force exists. This gives a finite and continuous stress at the crack tip.

4.2 Dynamic energy balance:-

Using the overall energy rate balance, the energy flux into the crack tip of an extending crack can be calculated. The analysis here follows Atkinson and Eshelby (1968) and Freund (1972). For simplicity, let us consider a plane crack (fig. 4.4) in a 2D deformation field, extending at an arbitrary rate ($\vec{v}$) where the figure represents the body at

a certain fixed instant of time.

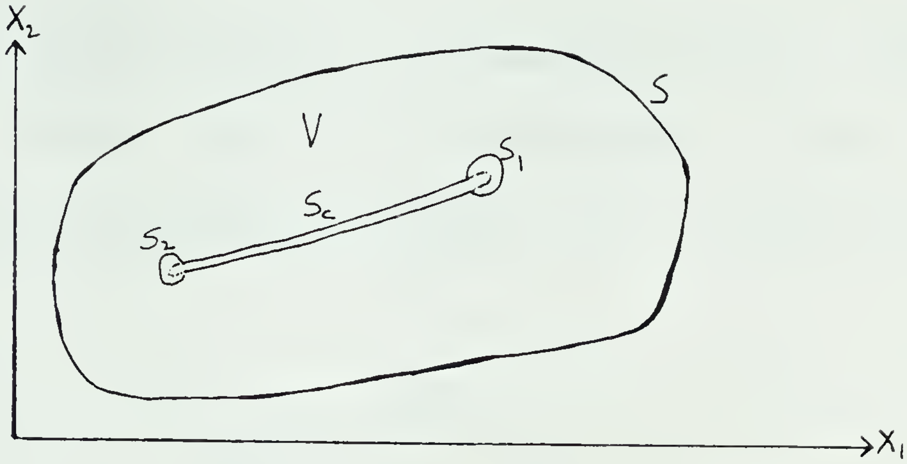

Fig. 4.4

Suppose that the crack is extending through the motion of either or both crack tips. At any instant of time, the rate of work (P) of the tractions on S is equal to the rate of increase of internal energy of the body plus rate at which energy is absorbed by the moving tip. By the body, is meant the region V in the limit as S_1 and S_2 shrink on to the crack tip. Denoting the total crack tip energy flux by $g = g_1 + g_2$ the energy rate balance is

$$P = \dot{U}_E + \dot{U}_K + g$$

Taking into the account that S_1 and S_2 move with the crack tip and expressing each term of the above equation in terms of elastic fields, we get:

$$g_\alpha = -\mathop{\mathrm{Lt}}_{S_\alpha \to 0} \int \left[\sigma_{ij} n_j \dot{u}_i + \left\{ \tfrac{1}{2} T_{ij} u_i + \rho \dot{u}_i \dot{u}_i \right\} v_n \right] ds \qquad 4.8$$

$$\alpha = 1, 2$$

where n_i is the normal to S_α directed away from the

crack tip.

Clearly the energy flux depends only on the near tip elastic field and the calculated value of g_α is independent of choice of contour S_α (Freund (1972) ,eq.

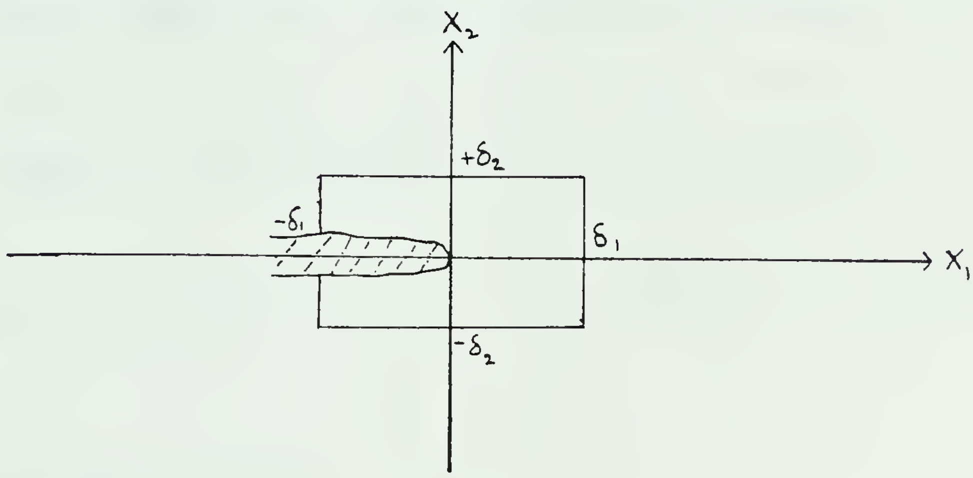

Fig. 4.5

14). Let $(\ell(t), t)$ be the position of the crack tip at any instant t, and choose S_α as a rectangular segment $|x_1 - \ell(t)| = \delta_1$ and $|x_2| = \delta_2$, where δ_1 and δ_2 are abritrarly small positive numbers. If the limit as $S_\alpha \to 0$ is interpreted as the ordered limit $\delta_2 \to 0$ followed by $\delta_1 \to 0$, then the only contribution to the integral in the equation 4.8 comes from the segments parallel to the x_1-axis, on which $v_n = 0$ and the equation 4.8 reduces to

$$g_\alpha = \lim_{\delta_1 \to 0} \int_{-\delta_1}^{\delta_1} \vec{T}(x_1', 0)\left[\dot{\vec{u}}(x_1', 0^+) - \dot{\vec{u}}(x_1', 0^-)\right] dx_1' \qquad 4.9$$

where $x_1' = x_1 - v t$

The energy flux (g) is related to the crack extention force (G) by,

$$g = 2 v G$$

where the factor 2 accounts for both faces of the crack. Using the equation 4.9 we find (Achenbach, 1974)

$$G = \frac{K^2}{\mu} A(v)\, B(v) \tag{4.10}$$

where $A(v)$ $B(v)$ are the functions only of the crack propagation velocity that decrease from a value near 1 at $v=0$ to zero at the terminal velocity. For anti-plane cracks

$$A(v) = (1 - v/v_s)^{1/2} \quad ; \quad B(v) = (1 + v/v_s)^{-1/2}$$

and for plane cracks

$$A(v) = S(-1/v)\,\frac{(1 - v/v_R)}{(1 - v/v_s)} \quad ; \quad B(v) = \frac{v_p/v_s}{2(v_p^2/v_s^2 - 1)}\,\frac{(1 + v/v_s)^{1/2}}{(1 + v/v_R)\, S(1/v)}$$

Here v_R is the Rayleigh wave velocity, and $S(p)$ is the de Hoop (1958) function defined as

$$S(p) = \exp\left[-\frac{1}{\pi}\int_1^{v_p/v_s} \operatorname{Tan}^{-1}\left(\frac{(\xi^2-1)((v_p/v_s)^2 - \xi^2)^{1/2}\,\xi^2}{(v_p^2/2v_s^2 - \xi^2)\qquad(\xi + v_p p)}\right) d\xi\right]$$

and the stress intensity K may be interpreted as the stress concentration that would remain if the crack suddenly stopped; it is a function only of the stress and extension history of the crack but it is independent of v (Fossum and Freund, 1975; Freund, 1976). As G is related to material

constant (Irwin criterion) so the equation 4.10 is also the equation of rupture velocity. Kostrov (1970) has developed following equation governing rupture velocity

$$2\Gamma = -\frac{\pi}{2\mu v_s^2 v R(1/v)}\left[\left(v^{-2}-v_p^{-2}\right)^{1/2} K_I^2 + \left(v^{-2}-v_s^{-2}\right)^{1/2} K_{II}^2\right] + \frac{\pi K_{III}^2}{2\mu v \left(v^{-2}-v_s^{-2}\right)^{1/2}} \qquad 4.11$$

where $R(p) = (2p^2 - v_s^{-2}) + 4p^2(v_p^{-2}-p^2)^{1/2}(v_s^{-2}-p^2)^{1/2}$

and subscript to the stress intensity factor term refers to the corresponding rupture mode. Here, a general situation involving all three modes of rupture is considered. Freund (1979) has given an extensive review on the mechanics of dynamic crack propagation.

4.3 Shear Cracks:-

Perhaps the simplest models for earthquakes are transient shear cracks. At time t=0 suddenly a crack appears at the origin and starts growing obeying the equation of motion

$$\frac{1}{v_s^2}\frac{\partial^2 u_2}{\partial t^2} = \frac{\partial^2 u_2}{\partial x_1^2} + \frac{\partial^2 u_2}{\partial x_3^2} \qquad 4.12$$

for anti-plane crack and

$$\rho\frac{\partial^2 u_1}{\partial t^2} = (\lambda+\mu)\frac{\partial \Delta}{\partial x_1} + \mu\nabla^2 u_1$$

$$\rho\frac{\partial^2 u_3}{\partial t^2} = (\lambda+\mu)\frac{\partial \Delta}{\partial x_3} + \mu\nabla^2 u_3 \qquad 4.13$$

$$\Delta = \frac{\partial u_1}{\partial x_1} + \frac{\partial u_3}{\partial x_3}$$

for plane crack, with the boundary conditions

$$\tau_{23} = -p(x_1,t) = \sigma^0_{23} - \sigma^d_{23} \qquad l_-(t) < x_1 < l_+(t) \quad ; x_3 = 0$$

$$u_2 = 0 \qquad x_1 < l_-,\ x_1 > l_+ \quad ; x_3 = 0 \tag{4.14}$$

for antiplane and

$$\tau_{13} = -p(x_1,t) = \sigma^0_{13} - \sigma^d_{13} \qquad l_-(t) < x_1 < l_+(t) \quad ; x_3 = 0$$

$$\tau_{33} = 0 \qquad \text{everywhere on } x_3 = 0 \tag{4.15}$$

$$u_1 = 0 \qquad x_1 < l_-,\ x_1 > l_+ \quad ; x_3 = 0$$

for plane crack, to-gether with the initial conditions

$$u_2 = \dot{u}_2 = 0 \qquad t \le 0 \tag{4.16}$$

for antiplane

$$u_1 = \dot{u}_1 = u_3 = \dot{u}_3 = 0 \qquad t \le 0 \tag{4.17}$$

for plane case.

Due to the symmetry w.r.t. the plane $x_3 = 0$ it is sufficient to find the solution only in one half-space. Hereafter the displacement on the crack plane will always refer to that determined for the half-space. The displacement discontinuity (slip) will be twice the surface displacement determined for the half-space.

Using Green's function technique, the integral equation for displacement is given by (Burridge, 1969)

$$u_n(x_1',0,t') = \int_{-\infty}^{+\infty} dt \int_{-\infty}^{+\infty} G_{ni}(x_1',0,t';x_1,0,t)\, \tau_{i3}(x_1,t)\, dx_1 \tag{4.18}$$

For anti-plane crack the Green's fuction for the half-space $X_3 \leqslant 0$ is given by (Achenbach, 1974)

$$G_{22} = \frac{H\left[(t'-t) - (x_1'-x_1)/v_s\right]}{\pi\mu\left[(t'-t)^2 - \{(x_1'-x_1)/v_s\}^2\right]^{1/2}} \tag{4.19}$$

With that, the solution is

$$u_2(x_1', 0, t') = \frac{1}{\pi\mu}\iint_{S_0} \frac{\tau_{23}(x_1, t)\, dx_1\, dt}{\sqrt{(t'-t)^2 - (x_1'-x_1)^2/v_s^2}} \tag{4.20}$$

where region S_0 of integration is the backwards characteristic triangle

$$|x_1' - x_1| \leq v_s\,(t'-t)$$

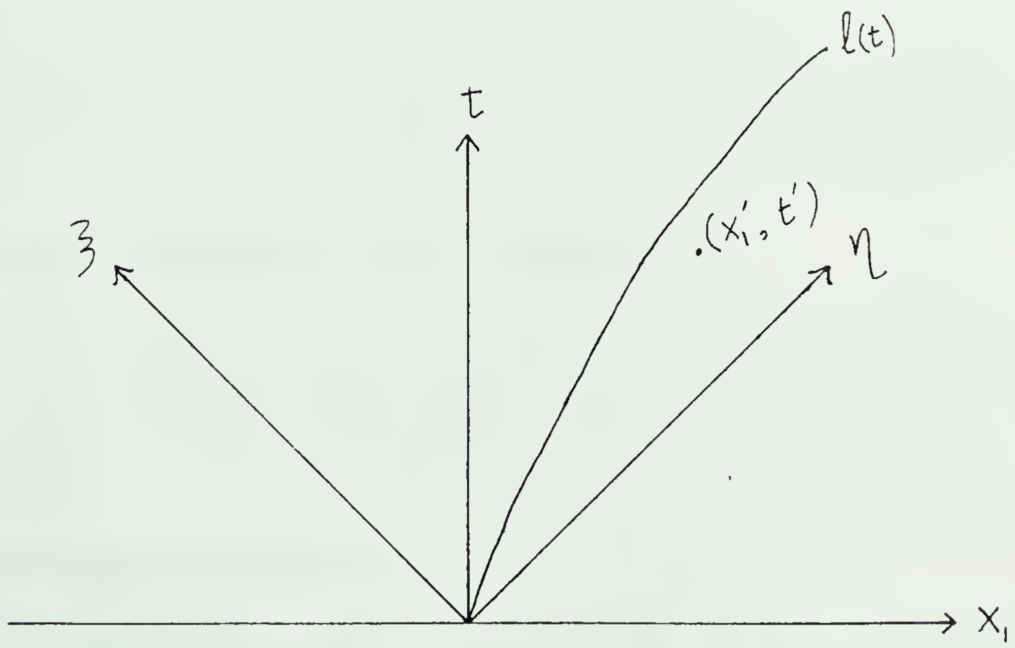

Fig. 4.6

Region S_0 may contain an area outside crack where τ_{23} is not known. So, to solve above equation, τ_{23} has to be found in that region. Kostrov (1966) has given it in terms of the stress drop p inside the crack assuming that a contribution comes only from one of the crack tips.

$$\tau(x_1', t') = \frac{1}{\pi\sqrt{x_1' - l(t_2)}} \int_{x_1' - v_s t'}^{l(t_2)} p[x_1, t' + (x_1 - x_1')/v_s] \frac{\sqrt{l(t_2) - x_1}}{(x_1' - x_1)}\, dx_1 \qquad 4.21$$

where $l(t)$ is the location of the crack tip and t_2 is the time when the crack tip locus intersects the integration path, namely

$$v_s t' - x_1' = v_s t_2 - l(t_2)$$

Considering the energetics at the crack tip, Kostrov gave the following equation governing the location of the crack tip

$$\int_{l - v_s t}^{l} p[x_1, t - (l - x_1)/v_s] \frac{dx_1}{\sqrt{l - x_1}} = (2\pi\mu G)^{\frac{1}{2}} \left(\frac{1 + \dot{l}(t)/v_s}{1 - \dot{l}(t)/v_s} \right)^{\frac{1}{4}} \qquad 4.22$$

The above equation holds only when

$$\int_{l - v_s t}^{l} p[x_1, t - (l - x_1)/v_s] \frac{dx_1}{\sqrt{l - x_1}} \geq (2\pi\mu G)^{\frac{1}{2}} \qquad 4.23$$

Using transformation

$$\xi_l = \{v_s t - l(t)\}/\sqrt{2} \quad ; \quad \eta_l = \{v_s t + l(t)\}/\sqrt{2} \qquad 4.24$$

The equation of the motion for the crack tip can be written as

$$\frac{d\xi_\ell}{d\eta_\ell} = \frac{(2\pi\mu G)^{1/2}}{\displaystyle\int_{\ell-v_3t}^{\ell} p[x_1, t-(\ell-x_1)/v_3]\frac{dx_1}{\sqrt{\ell-x_1}}} \qquad 4.25$$

Once the locus of the crack tip is determined τ_{23} can be calculated and the displacement field on $x_3=0^-$ is, using a transformation similar to 4.24, given by

$$u_2(\xi',\eta') = -\frac{1}{\sqrt{2}\,\pi\mu}\int_{\xi_\ell(\eta')}^{\xi'}\frac{d\xi}{\sqrt{\xi'-\xi}}\int_{-\xi}^{\eta'}\frac{p(\xi,\eta)\,d\eta}{\sqrt{\eta'-\eta}} \qquad 4.26$$

Thus the displacement discontinuity or slip will be $(-2u_2)$ and the slip velocity (Achenbach, 1974)

$$\Delta\dot{u}_2(x_1,t) = \frac{2}{\pi\mu}\frac{v}{(1+v/v_3)^{1/2}(vt-x_1)^{1/2}}\int_0^{\ell(t)}\frac{p[x_1, t-(\ell(t)-x_1)/v_3]}{\sqrt{\ell(t)-x_1}}\,dx_1 \qquad 4.27$$

Madariaga (1977), using the above equations, did calculations for the elastic field with $v = 0.5v_3$ (fig.

4.7).

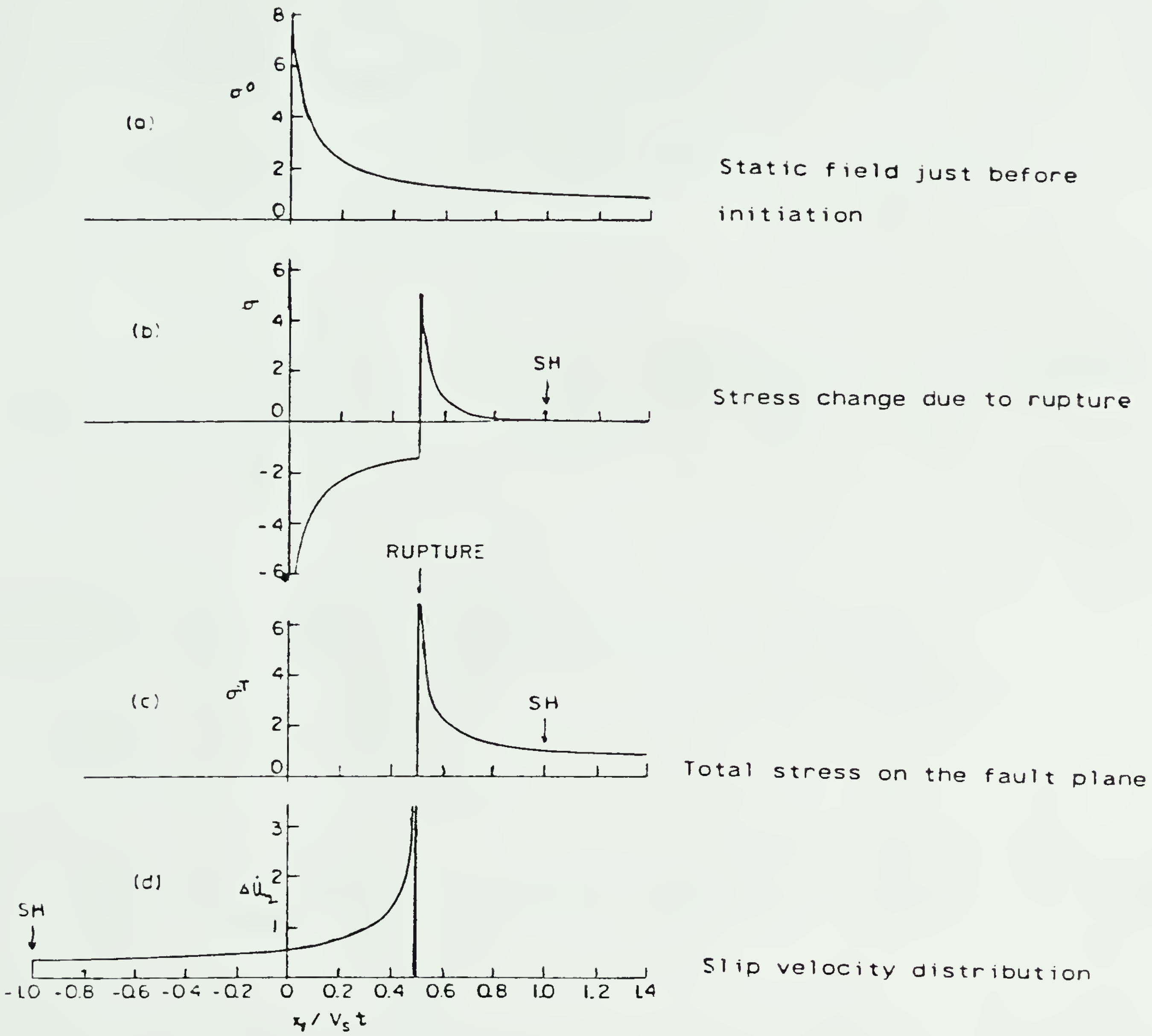

Fig. 4.7 Elastic field on the plane of suddenly starting anti-plane crack (Madariaga, 1977).

For in-plane we have the solution

$$u_1(x_1', 0, t') = \iint_{S_0} G_{11}(x_1', 0, t'; x_1, 0, t)\, \tau_{13}(x_1, t)\, dx_1\, dt$$

4.28

$$u_3(x_1', 0, t') = \iint_{S_0} G_{13}(x_1', 0, t'; x_1, 0, t)\, \tau_{13}(x_1, t)\, dx_1\, dt$$

and the Green's functions given by Lamb (1904) are as follows.

$$G_{11}(X_1,0,t) = \frac{4\alpha^2}{\pi\mu v_s^2 X_1} \frac{(\alpha^2 - v_s^{-2})(\alpha^2 - v_p^{-2})^{\frac{1}{2}}}{R(\alpha)\, R^*(\alpha)} \qquad \frac{1}{v_p} < \alpha < \frac{1}{v_s}$$

$$= \frac{1}{\pi\mu v_s^2 X_1} \frac{(\alpha^2 - v_s^{-2})^{\frac{1}{2}}}{R(\alpha)} \qquad \frac{1}{v_s} < \alpha$$

4.29

$$G_{13}(X_1,0,t) = \frac{K_\ell}{\mu}\,\delta(t - X_1/v_R) + \frac{2\alpha}{\pi\mu v_s^2 X_1} \frac{(2\alpha^2 - v_s^{-2})(\alpha^2 - v_p^{-2})^{\frac{1}{2}}(v_s^{-2} - \alpha^2)}{R(\alpha)\quad R^*(\alpha)}$$

where $\alpha = \frac{t}{X_1}$, and R is the Rayleigh function

$$R(\alpha) = (2\alpha^2 - v_s^{-2})^2 - 4\alpha^2(\alpha^2 - v_p^{-2})^{\frac{1}{2}}(\alpha^2 - v_s^{-2})^{\frac{1}{2}}$$

$$R^*(\alpha) = (2\alpha^2 - v_s^{-2})^2 + 4\alpha^2(\alpha^2 - v_p^{-2})^{\frac{1}{2}}(\alpha^2 - v_s^{-2})^{\frac{1}{2}} \qquad 4.30$$

and K_ℓ is defined by

$$K_\ell = \frac{\left(2(v_s/v_R)^2 - 1\right)^3}{16(v_s^2/v_R^2)\left[1 - (6 - 4(v_s^2/v_p^2))(v_s^2/v_R^2) + 6(1 - (v_s^2/v_p^2))(v_s^4/v_R^4)\right]} \qquad 4.31$$

S_0, the area of the integration, is backwards characteristic triangle

$$|X_1' - X_1| \leq v_p(t' - t)$$

which has region lying outside the crack for which τ_{13} is

not known. Similar to the anti-plane crack Kostrov (1975) obtained the analytic solution using integral transforms and Wiener-Hopf technique. The results are much more complicated than the anti-plane case and valid only for $v < v_R$. Madariaga's (1977) calculations based on those results are reproduced here (fig. 4.8)

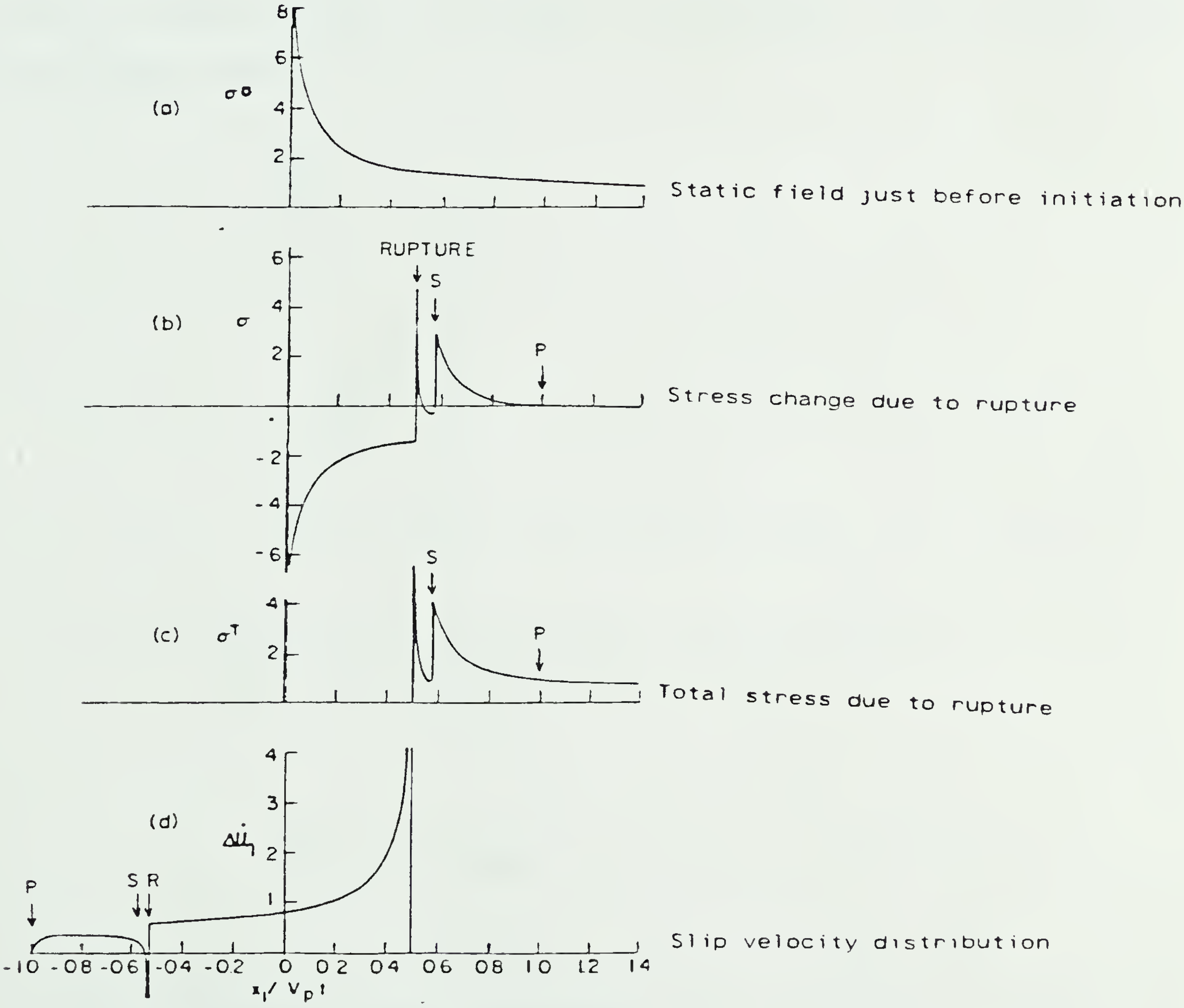

Fig. 4.8 Elastic field on the plane of suddenly starting in-plane crack (Madariaga, 1977).

Slip dependent boundary condition:-

A gradual creep deformation prior to the sudden motion on the fault is observed in the field as well as in the laboratory experiments. Ida (1973) suggested a constitutive relationship between stress and slip rate to be incorporated in the solution of the crack propagation to take into the account creep motion. He gave an analysis only for the anti-plane case.

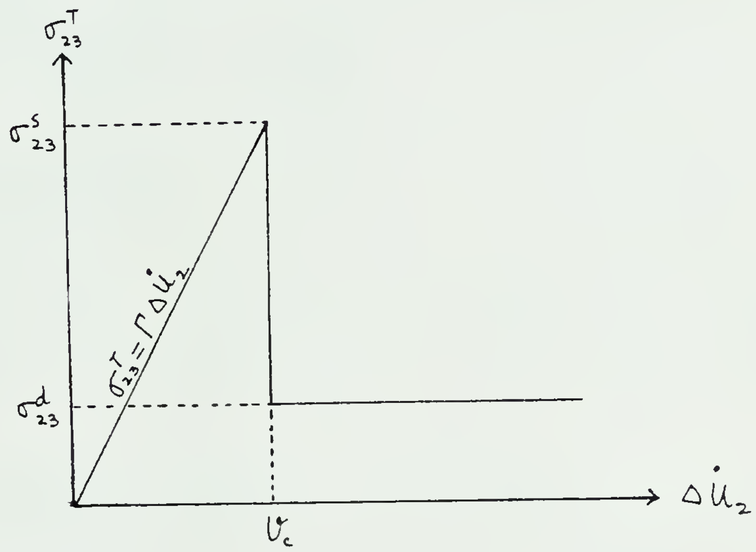

Fig. 4.9 Constitutive relation between stress and slip rate (Ida, 1973). ϑ_c is critical slip rate.

$$\begin{aligned} \sigma_{23}^{T} &= \Gamma\Delta\dot{u}_2 & \quad \Delta\dot{u}_2 < \vartheta_c \\ &= \sigma_{23}^{d} & \quad \Delta u_2 > \vartheta_c \end{aligned} \tag{4.32}$$

As tectonic stress increases over dynamic frictional stress (σ_{23}^{d}) creep motion starts along the fault plane and the rate of slip increases with the stress increase till it reaches a critical (static frictional stress) value, beyond

that stress drops to the level σ_{23}^{d} creating an earthquake.

Let us consider that a semi-infinite crack suddenly appears for $x_1 < 0$ at $t=0$. Thus, there will be two time intervals $t < -\frac{x_1}{v_s}$ and $t > -\frac{x_1}{v_s}$. For $t < -\frac{x_1}{v_s}$ there will not be any disturbance from the crack tip so during that period the slip will be uniform and the stress drop will be determined by the constitutive relation 4.32.

The displacement field is obtained by integrating (4.26) over appropriate limits and yields

$$u_2 = -\frac{v_s p t}{\mu}$$

Using relation 4.32

$$\sigma_{23}^{T} = \sigma_{23}^{0} + \tau_{23} = \sigma_{23}^{0} - p = \Gamma \Delta \dot{u}_2 = -2\Gamma \dot{u}_2 = 2\Gamma v_s p/\mu$$

$$\text{for } t < -x_1/v_s$$

Thus the stress drop in terms of initial stress and material constant is

$$p = p_0 = \frac{\sigma_{23}^{0}}{1 + \Gamma v_s/\mu} \tag{4.33}$$

For $t > -x_1/v_s$ we have disturbances coming from the crack tip, so both p as well as u_2 are unknown and the solution can be obtained by solving both 4.26 and 4.32 simultaneously. To solve it Ida (1973) developed a numerical scheme based on discretization of integral equation.

For various choice of parameters v_c , Γ and σ_{23}^{d} Ida made numerical calculation and found that there are two distinct classes of rupture; in one of them rupture once started, accelerates smoothly to v_s (fig. 4.10) and in the another class rupture after propagating comes to rest, then restarts, stops, and repeats the process (fig. 4.11).

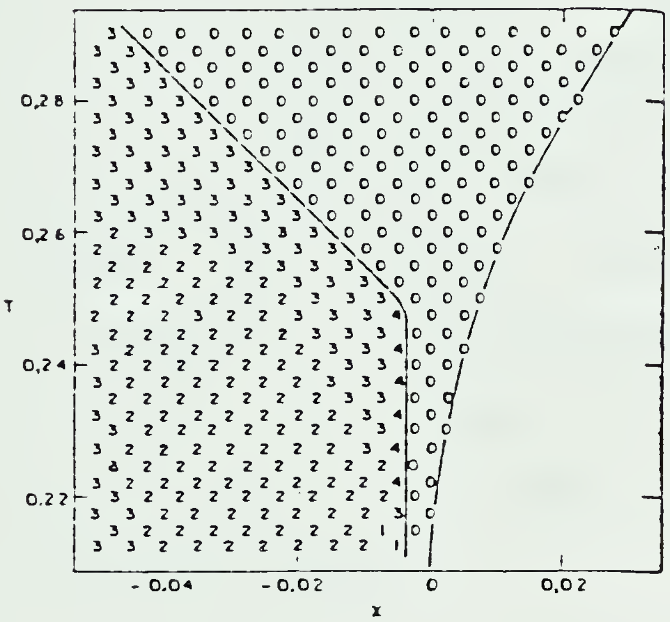

Fig. 4.10 Smooth rupture propagation (Ida, 1973).

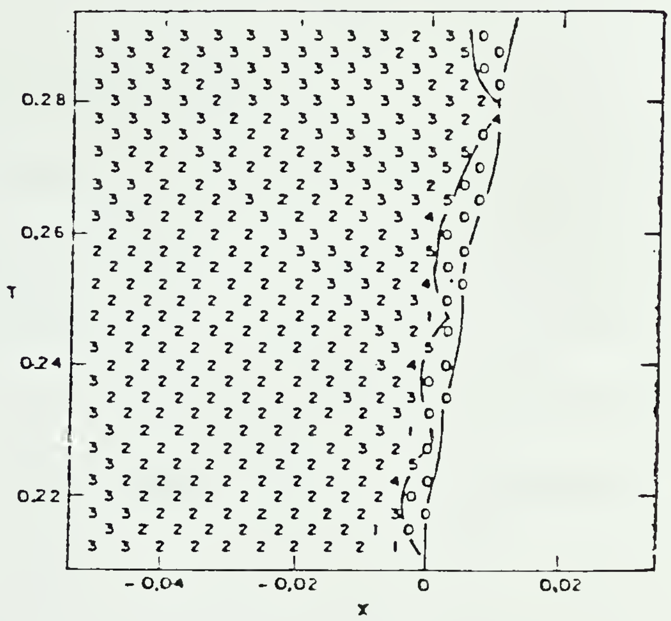

Fig. 4.11 Irregular rupture propagation (Ida, 1973).

Distribution of σ_{23} in the unit of p_0 . Time is measured in the unit of t_0 and distance in the unit of $v_s t_0$. Where is the time required for crack initiation $(\pi \mu G / 2 v_s^2 p_0^2)$.

Andrews (1976), for in-plane cracks similar to Ida's, developed a slip weakening model assuming that the shear

$$\sigma(\Delta u) = \sigma^s - (\sigma^s - \sigma^d)\Delta u / d \qquad \Delta u < d \tag{4.34}$$

$$= \sigma^d \qquad \Delta u > d$$

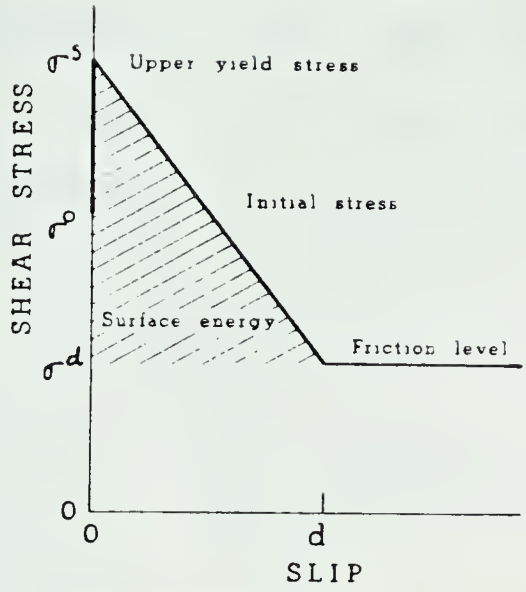

Fig. 4.12 Slip weakening model (Andrews, 1976).

stress across the crack plane is a function of the slip and when the stress reaches the static friction limit, instability begins and weakening occurs. For slip greater than d, the stress drops to the dynamic friction and the work done up to that point is identified as specific fracture energy,

$$G = \frac{1}{4}(\sigma^s - \sigma^d)\,d$$

With this model he examined the rupture propagation by a finite difference scheme. The results are dicussed in terms of two nondimensional numbers, L_c/L and $S = \dfrac{\sigma^s - \sigma^0}{\sigma^0 - \sigma^d}$, where σ^0 is the initial stress and L_c is the critical half length of the in-plane Griffith crack which is given by

$$L_c = \frac{8\mu(\lambda+\mu)G}{\pi(\lambda+2\mu)(\sigma^0-\sigma^d)^2}$$

The calculation shows that when the parameter S is greater than 1.63, then ϑ is always less than ϑ_R, and ϑ approaches ϑ_R as the crack length increases.

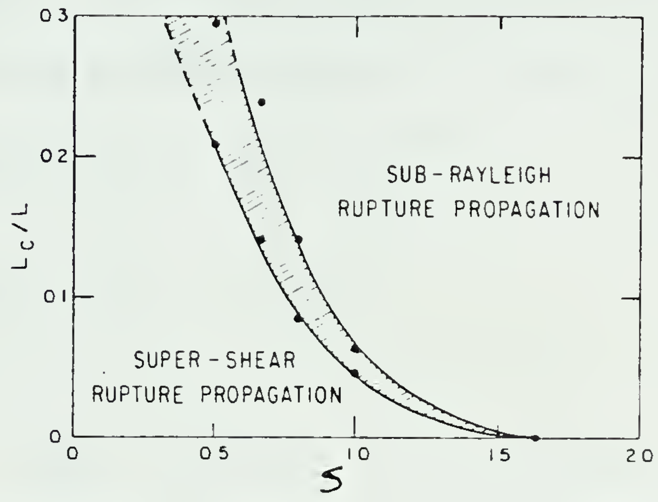

Fig. 4.13 Rupture propagation with slip weakening model (Andrews, 1976).

But for $S = 1.63$ the crack is accelerated towards ϑ_S and may approach ϑ_P as the crack length increases. The range $\vartheta_R < \vartheta < \vartheta_S$ appears to be forbidden. Burridge (1979) has also confirmed this forbidden range.

<u>Stopping mechanism of the cracks:-</u>

Husseini (1975) suggested that along trajectory of a running crack either an increase in fracture energy or finiteness of available strain energy will arrest the propagation of the crack. An example of the former situation may be a rupture initiating on pre existing fault locked by frictional stress and attempts to propagate into the region of fresh unfractured rock possesing greater fracture energy.

And a region in the path incapable to supply any stress drop to the crack when the crack-tip passes them, might be an example to the latter case. For semi infinite anti-plane crack Husseini examined these mechanisms and found that if arrest is through the presence of fracture energy barriers then the inequality to be satisfied is

$$(\Gamma + \Delta\Gamma) \geqslant \frac{2R\,\Delta\sigma^2}{\mu\pi} \tag{4.35}$$

where $\Delta\Gamma$ is the increase in fracture energy, $\Delta\sigma$ is the average stress drop and R is the characteristic radius of the fault.

If on the other hand the earthquake is arrested according to the finiteness of strain energy or seismic gap model then

$$\Gamma = \frac{R\,\Delta\sigma^2}{2\mu\pi} \tag{4.36}$$

Thus if arrest is predominantly caused by barriers then the the inequality 4.35 will constitute a weak relationship between the fracture energy, stress drop and radius. If, on the other hand, arrest is caused by seismic gaps, equation 4.36 constitutes a strong relationship between fracture energy, stress drop and radius. Interestingly both 4.35 and 4.36 predict that the fracture energy will be proportional to the radius and the square of the stress drop.

The equation 4.36 leads to the following relationship,

$$\log \Delta\sigma = -\frac{1}{2}\log R + \frac{1}{2}\log(2\mu\pi\Gamma)$$

The combination of this relationship with the Keilis-Borok (1959) relationship between stress drop and seismic moment (M) yields,

$$\log M = \frac{5}{2}\log R + \frac{1}{2}\log(2\mu\pi\Gamma) + 0.64$$

This relationship is statistically acceptable for the Southern California faults and the Tonga-Kermadec Arc earthquakes suggesting that the seismic gap model of arrest may be valid in those regions.

Andrews (1975) applied numerical methods to the two dimensional shear cracks problem and found that with an appropriate nonuniform initial shear stress the crack would stop by itself.

Radiation field of the crack model:-

Richards (1973,76) solved the problem of a 3D prestressed medium in which the rupture front starts at a point and propagates out as an ellipse over the fault surface at constant velocity. From the consideration of the stress near the fault surface, he concluded that the rupture velocity will be between v_R and v_s . The synthetic

seismograms calculated by him are reproduced below (fig. 4.14).

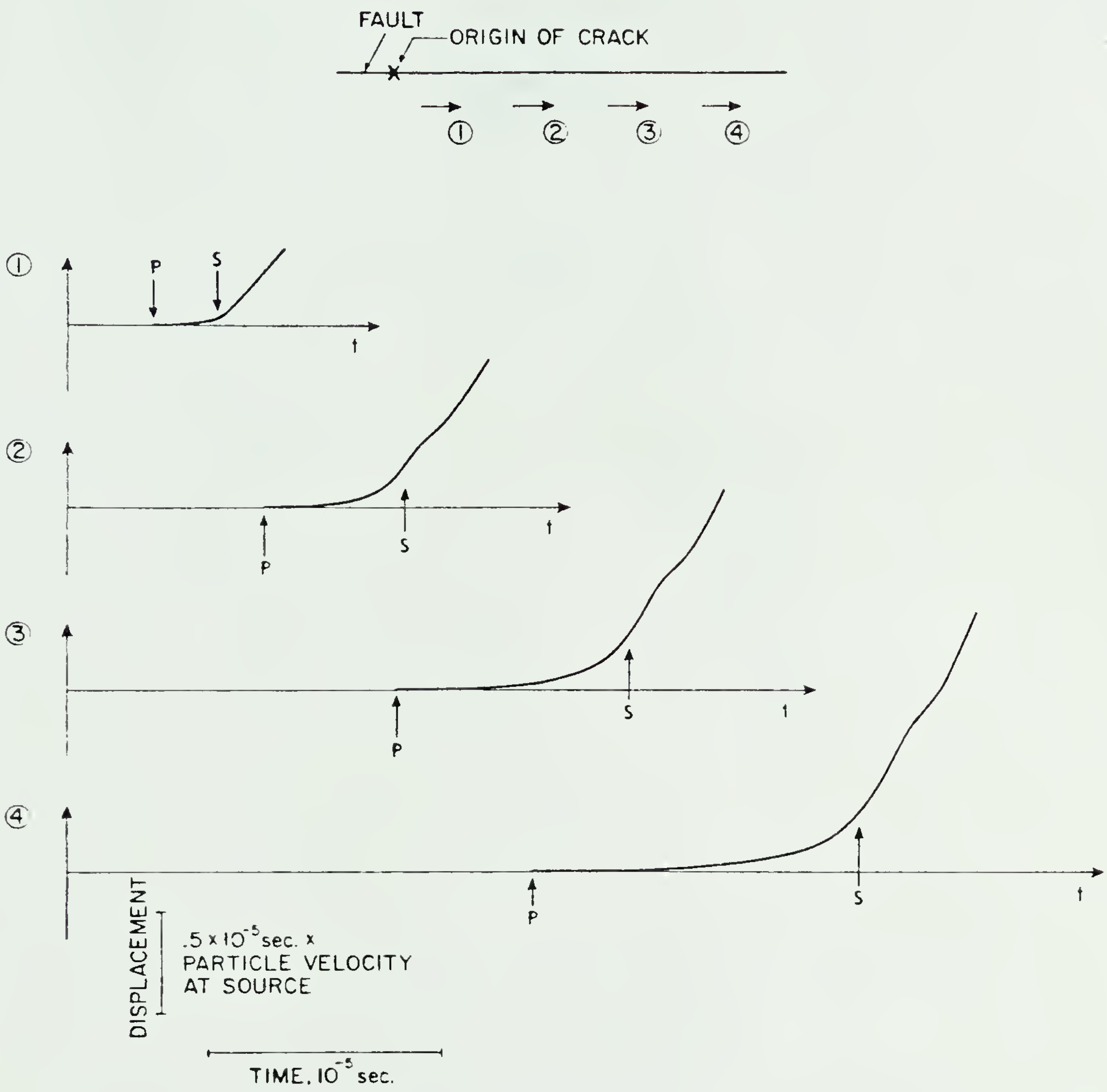

Fig. 4.14 Synthetic seismograms due to elliptical rupture (Richards, 1976).

Madariaga (1976) also applied numerical methods to a plane circular crack in 3D which expands at a prescribed constant velocity and then suddenly stops. The solution for slip on the fault and far field body waves were obtained (fig. 4.15). The far field displacements were strongly affected by the energy radiated when the fault stopped.

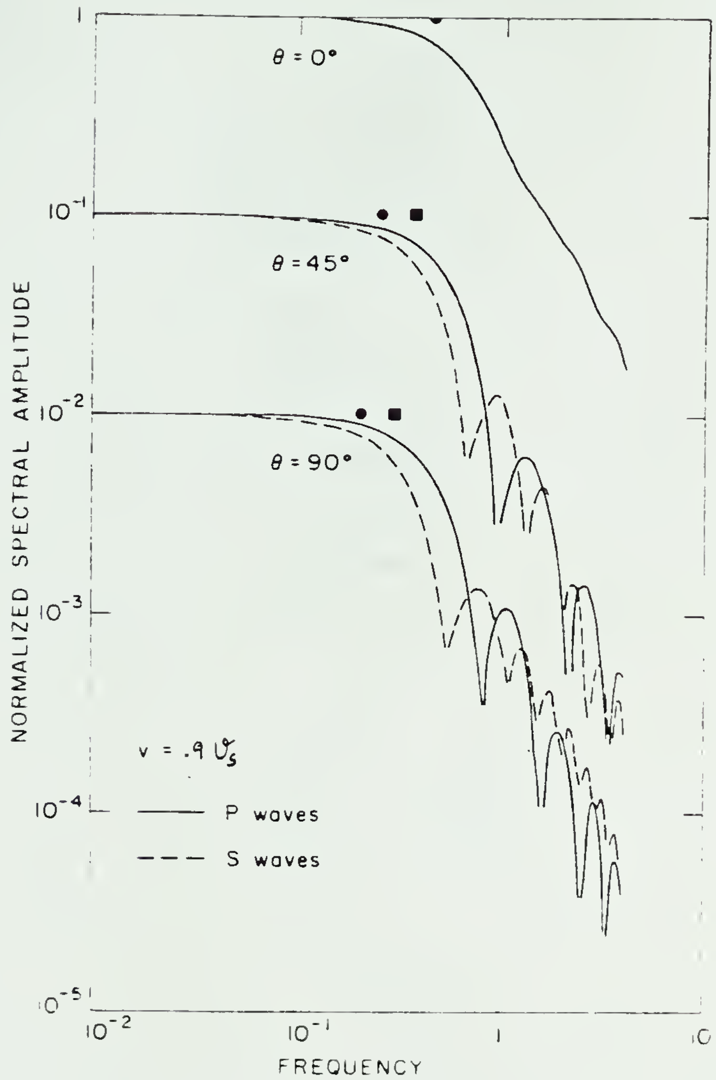

Fig. 4.15 Far field spectra for P and S waves due to circular crack (Madariaga, 1976).
θ is the take-off angle (angle between x_3-axis and direction of observation).

On further investigation Madariaga (1977) found that due to the sudden starting or stopping, high frequencies are radiated from the fault and are determined by the change in the slip velocity field. Since the highest slip velocities occur right behind the rupture front, it is expected that these radiations come from the region in the neighbourhood of the crack-tip. The radiation pattern due to the sudden starting or stoping of a shear crack is shown in the figure 4.16. Aki(1980) has presented an extensive review on dynamic

source theory.

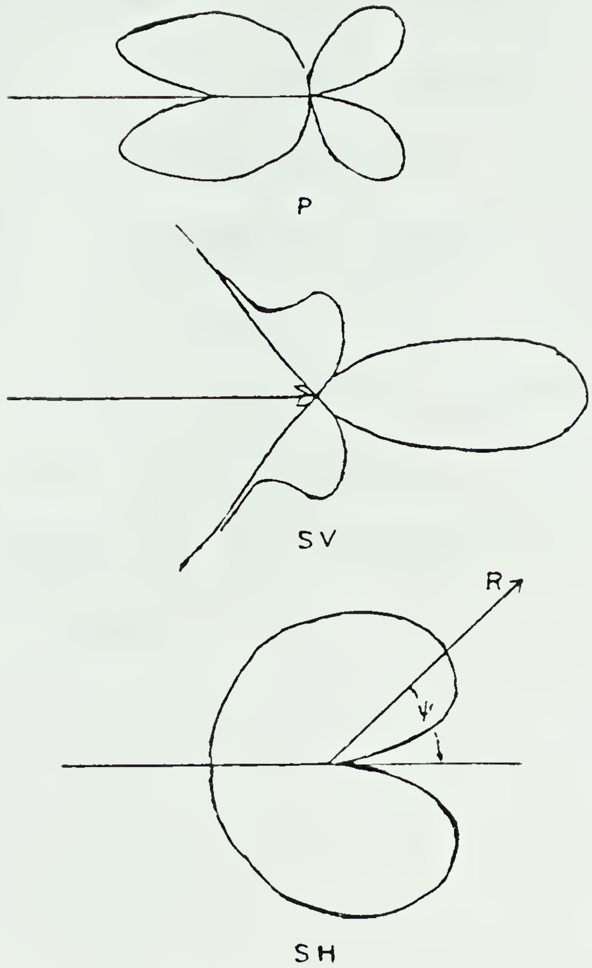

Fig. 4.16 Radiation pattern from the suddenly starting or stopping in-plane crack (P and SV waves) and anti-plane crack (SH wave) (Madariaga, 1977).

It may be pointed out that the validity of the result presented here is much restricted for a real earthquake due to the simplifying assumptions considered . The assumptions are

1. an unbounded solid
2. homogeneous, isotropic, linear elastic material
3. a plane two dimensional geometry
4. extension of crack in its own plane
5. constant value of Γ
6. brittle fracture

Obviously it will be desirable to remove some of the restricting assumptions. In particular, since it has been observed in the field that faults may bifurcate, an extension of the analytical work to include branching and asymmetric crack propagation deserve primary attention. Extension of analytical work to include interactions between the tip of the crack is also of interest. Also the plastic flow in conjuction with dynamic fracture and possible functional dependence of Γ on rupture velocity should also be the subject of study.

5. SIMULATION OF FAULT MOTION AND EARTHQUAKE OCCURRENCE

There have been attempts to simulate the fault motion and the occurrence of earthquakes by experimental as well as by numerical means. Generally it is accepted that faulting associated with earthquakes is related to the relative sliding of two rock surfaces with frictional resistance opposing the motion. In the simulations, the fault regions are repesented by discrete blocks which are driven to slide on the friction surface by various combinations of elastic and viscous force elements.

In the experiments on rock friction it has been found that there are two modes of displacement along a frictional surface; stable, in which there is continuous displacement without abrupt change in the applied force, and stick slip which is a jerky motion. Under the varying condition of normal stress, displacement rate, pressure, temperature, pore fluid etc. both occur. Also transition from one mode to another takes place but this is not usually abrupt. At low pressure, say 10 bars, the sliding mode is seen to be stable and changes to stick slip at higher pressure. With increase of temperature, due to ductile flow the transition from stable to stick-slip is inhibited. It has been observed in sandstones that with the increase of velocity a transition from stick-slip to stable takes place. Also higher pore

fluid pressure promotes stable sliding (Logan, 1975).

The motions on the fault surface are found to take place suddenly. During the sudden slip, shear stresses are relieved and the fault surface may thus remain locked together until some time later slip suddenly takes place again. Such sudden intermittent motion on a pre-existing fault in the earth is similar to jerky sliding between the rock surface in laboratory experiments (Brace & Byerlee, 1966). Therefore stick slip is consider to be a possible mechanism of slip along the fault. The assumption made to explain stick-slip is the fact that dynamic friction is less than static friction. The physical basis put forward for this are: thermal softening, creep instability and brittle failure. Byerlee (1970) examined these alternatives in detail and suggested that the most probable cause may be brittle failure.

It has been observed that there is an increase of temperature at the sliding surfaces. Since a rise of temperature lowers the strength of material, this leads to the idea that friction during sliding,i.e., dynamic friction may be less than static friction. If this is the only cause, then before stick slip starts there should be always a period of stable slip during which temperature rises to decrease the strength of material. This is not true.

When surfaces are held to-gether they make contact only at a few points. The creep instability model assumes that

these points of contact or junctions deform by creep mechanism so that the size of the junctions increase with time. During the sliding, the time of contact is so small that junction growth does not occur. If the friction force is the force required to shear the junctions then the force required to start sliding after the block has been at rest may be greater than the force required to maintain sliding. Hence static friction could be greater than dynamic friction. Dieterich (1972a) has observed this effect and concludes

$$\mu(t) = \mu(0)\left[1 + \alpha \log \Delta t\right] \qquad \Delta t > 1 \text{ Second} \tag{5.1}$$

where α is a constant and is the duration of the contact following sliding. Recently on the basis of the laboratory data he (Dieterich, 1979) has developed the following quantitative relationship between cofficent of friction μ and time of stationary contact and slip velocity $\dot{u}(t)$.

$$\mu(t) = \left[C_1 + C_2 \log(C_3 \Delta t + 1)\right]\left\{f_1 + \frac{1}{f_2 \log\left[(f_3/\dot{u}) + 10\right]}\right\} \tag{5.2}$$

where $C_1, C_2, C_3, f_1, f_2, f_3$ are constants.

The brittle instability model for stick-slip considers that asperities along the fault surface lock together to form the frictional resistance. When the shear force becomes strong enough to cause brittle failure of these asperities, motion can occur. As the sliding proceeds, continual locking and breaking of asperities causes fluctuations in the

frictional resistance. Thus the frictional resistance varies in some irregular manner with displacement. The value of frictional resistance at the initiation of an unstable sliding event is analogous to the static friction, and the average value of fluctuating friction during the sliding corresponds to dynamic friction (Nur and Shultz (1973), Nur (1978)). The presence of gouge along a sliding surface is strong evidence in the favour of this brittle instability mechanism of stick-slip.

The modeling of fault motion also requires some relationship between the stress acting on the rocks and the consequential strain . In general this relationship can be quite complicated, but even by restricting the analysis to a linear relation between them, considerable understanding of the process can be had. Thus for a connecting element of the model, the stress-strain relationship can be written as

$$\sigma = O\dot{\epsilon}$$

where O is a linear operator on $\dot{\epsilon}$.

For an elastic spring, $O\dot{\epsilon} = k\int\dot{\epsilon}\,dt = k\epsilon$,while for a viscous element, $O\dot{\epsilon} = \eta\,\epsilon$ (Jaeger and Cook, 1976).

More complicated connecting elements can be constructed by the combination of these simple elements, and applying linear operator techniques, stress-strain relationship can be derived (fig. 5.1a). The time dependent behaviour of stress and strain for those substances is shown in the fig. 5.1b.

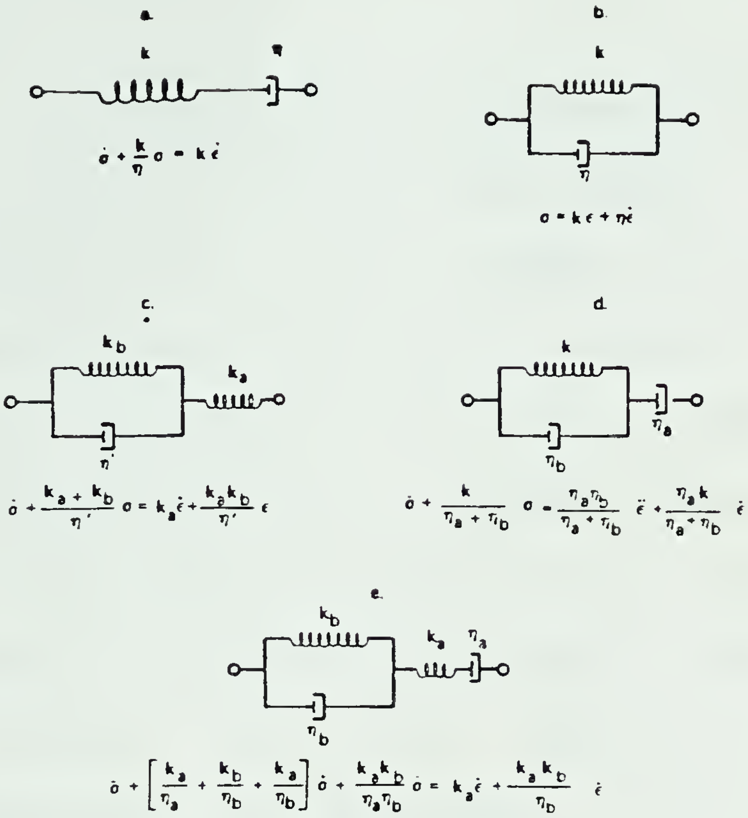

Fig. 5.1a Multiple-element rheologic model (Cohen, 1979)

(a) Maxwell substance

(b) Kelvin substance

(c) Three element generalized Kelvin

(d) Alternative three element substance

(e) Four element Burgers substance.

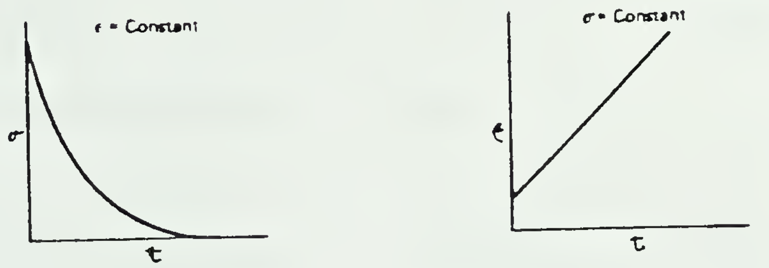

Maxwell substance

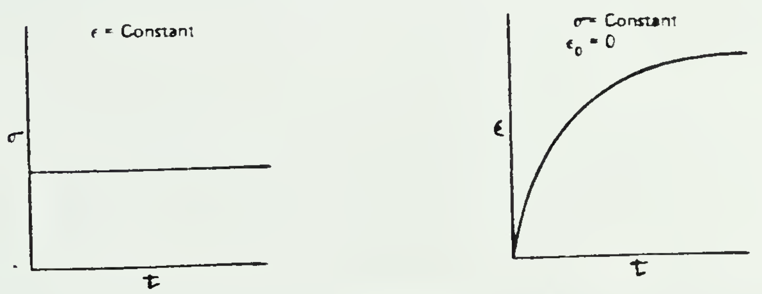

Kelvin substance

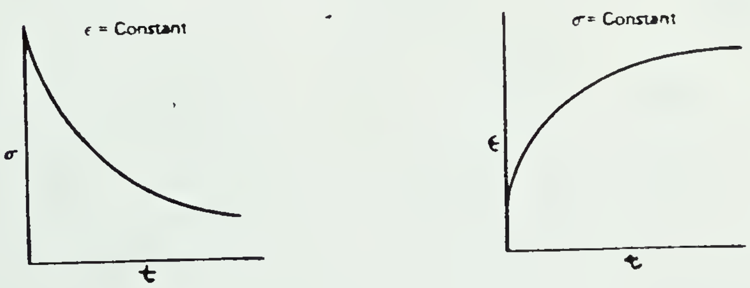

Generalized Kelvin substance

Fig. 5.1b

Time dependent behaviour of stress and strain for selected linear substance (Cohen, 1979).

5.1 Simulation models for earthquakes:-

Different authors have tried to stimulate stick-slip by the help of mechanical models. These models can be categorized into two classes: the first consists of a mass, sliding over a frictional surface, driven by a constant force applied on the block through a spring (Rider model), another consists of a linear array of masses conected via spring elements and driven by springs conected to a moving plate (Burridge and Knopoff model). Assuming different friction laws and rheological models for connecting elements, the equations of motion of the blocks are constructed and then rupture velocity, time of slide, frequency of slide etc. are calculated. These results are then matched with natural events. With these some authors have also constructed laboratory models. A systematic detail of different models is presented below.

Rider model:-

Rider model consists of a mass spring system as shown in (fig. 5.2). A block of mass m sitting on a rigid frictional surface is subjected to stress due to accumulation of elastic strain within a spring which is being stretched at constant velocity V. In absence of any inertial motion in the block, the friction force prevents

any sliding until the stress rises to the maximum strength f^s. Once sliding has begun, the friction resistance drop to the dynamic value f^d, which tend to accelerate the block. This results in a decrease of force in the spring and

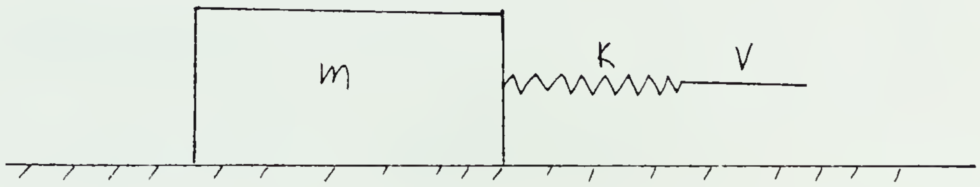

Fig. 5.2 Rider model.

the block eventually stops. Now the block remains stationary until the forces in the spring once again build-up to a value to overcome friction forces.

Assuming the initial position of the block is at $X=0$, motion is initiated at a time t_o when

$$K V t_o = f^s \tag{5.3}$$

and then block starts moving; the equation of motion of the block can be written as

$$m\ddot{u} = K(Vt - u) - f^d \tag{5.4}$$

the solution of above equation is

$$u(t) = \frac{(f^s - f^d)}{K}\left\{1 - \cos\left(\frac{K}{m}\right)^{\frac{1}{2}}(t - t_o)\right\} + V(t - t_o) - V\left(\frac{m}{K}\right)^{\frac{1}{2}}\sin\left(K/m\right)^{\frac{1}{2}}(t - t_o)$$

For practical purposes, once the sliding starts, the block begins to move much faster than V, so we can neglect the effect of V in the equation 5.4. This is equivalent to setting $t=t_0$ in the equation 5.4. Thus we have,

$$m\ddot{u} + Ku = KVt_0 - f^d = f^s - f^d = \Delta f$$

and the solution is

$$u \approx \frac{\Delta f}{K}\left(1 - \cos\left(\frac{K}{m}\right)^{\frac{1}{2}}(t - t_0)\right) \qquad 5.5$$

so we have velocity of the block

$$\dot{u} = \frac{\Delta f}{\sqrt{Km}} \sin\left(\frac{K}{m}\right)^{\frac{1}{2}}(t-t_0) \qquad 5.6$$

and the acceleration

$$\ddot{u} = \frac{\Delta f}{m} \cos\left(\frac{K}{m}\right)^{\frac{1}{2}}(t-t_0) \qquad 5.7$$

Duration of slip is obtained by setting $\dot{u}(t_1)=0$ in 5.6

$$(t_0 - t_1) = \Delta t = \pi\sqrt{m/K}$$

Total displacement

$$\Delta u = \frac{2\Delta f}{K}$$

Force drop

$$\Delta F = \Delta u \cdot K = 2\Delta f$$

Peak velocity

$$\dot{u}_{max} = \frac{\Delta f}{\sqrt{Km}}$$

Peak acceleration

$$\ddot{u}_{max} = \Delta f/m$$

and Potential Energy drop

$$\Delta E = f^d \Delta u = \frac{2}{K} f^d \Delta f = \frac{2}{K} f^d (f^s - f^d)$$

Although this model is an oversimplification of complicated tectonic and geologic processes, it is still able to give a qualitative picture of the fault motion.

Nur (1978) introduced non uniform friction in the equation of motion of the rider model to incorporate the brittle instability mechanism. Since in the rider model there is no distiction between displacement or position, therefore let $f(x)$ be a position dependent function representing non uniform friction. Then the equation of motion of the rider can be written as

$$m\ddot{u} + Ku = f(x)$$

with initial conditions

$$u(0) = x_0 \quad , \quad \dot{u}(0) = V$$

and we get expression for time of the rider at any position

$$t = \int_{x_0}^{x} \frac{dx}{V^2 + 2\int_{x_0}^{x}\left(-K/m\, x + \frac{f(x)}{m}\right)dx}$$

On inverting above equation one gets the displacement time function $u(t)$.

In the derivation of the above equation the nature of non-uniform friction is not specified. Thus depending upon the nature of $f(x)$, a solution will be obtained either by analytical or numerical means.

Whitehead & Gans (1974) have examined the behaviour of

the rider model with the assumption that the rider and sliding surface are separated by a thin temperature dependent viscous layer so that the net friction forces decrease with increasing velocity and the solution obtained shows violent motion over a small period of time followed by a quiet period.

The most detailed quantitative calculation on rider model has been done with variable friction and a viscoelastic element by Cohen (1978). The introduction of this element permits modeling of the transient anelastic deformation in response to stress loading and relaxation, and provides a mechanism for partial stress recovery following an earthquake. As a consequence, it is possible to simulate the episode of stable sliding, tertiary creep preceeding earthquake and long term aseismic creep also.

Burridge and Knopoff Model:-

There has been another independent effort to formulate dynamical equation for particle displacement on a fault by Burridge and Knopoff (1967). This consists of a number of masses connected together by springs and resting on a frictional surface. The masses are driven by springs connected to a moving plate (fig. 5.2). The various springs corresponds to elastic and viscous properties of the material. The driving plate is moving with velocity V

which is unaffected by the frictional resistance along the fault. Let F_i be the elastic force acting on the ith block which is associated with static friction f_i^s.

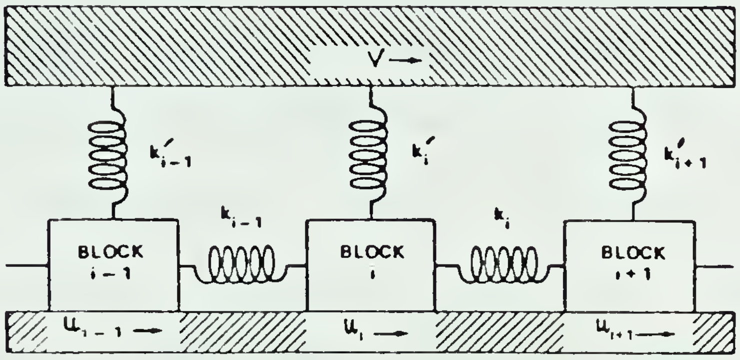

Fig. 5.3 One dimensional Burridge and Knopoff model.

Initially all blocks are at rest and $F_i < f_i^s$ for each block. As time advances, F_i grows due to the motion of the driving block which increases the driving spring tension. Once F_i overcomes the frictional resistance the motion of block i starts. This is governed by the following equation

$$m_i \frac{d^2 u_i}{dt^2} = F_i - f_i^d$$
$$= K_i (u_{i+1} - u_i) + K_{i-1} (u_{i-1} - u_i) + K_i' (Vt - u_i) - f_i^d \qquad 5.8$$

Here

m_i = mass of i'th block

K_i = spring constant for the spring connecting blocks i and i+1

K_i' = spring constant for the spring connecting i'th blocks and the driving plate

f_i^d = dynamic friction resistance of the i'th block

u_i = displacement of the i'th block

As the block slides, it compresses or expands the connecting springs to the adjacent blocks and possibly stimulates the motion of these blocks. In this manner slip will propagate along the fault. Thus the motion is governed by a set of coupled dynamic equations which can be solved by numerical techniques. Taking different numbers of blocks, different values of masses, different rheological elements and friction laws, many authors have examined this model (Burridge and Knopoff (1967), King and Knopoff (1968), King(1975),Otsuka (1972), Dieterich (1972b,73), Cohen (1977), Rundle and Jackson (1977)).

The one dimensional model for laboratory studies of Burridge and Knopoff (1967) consists of eight mass connected by a spring and driven by stretching of the spring connected

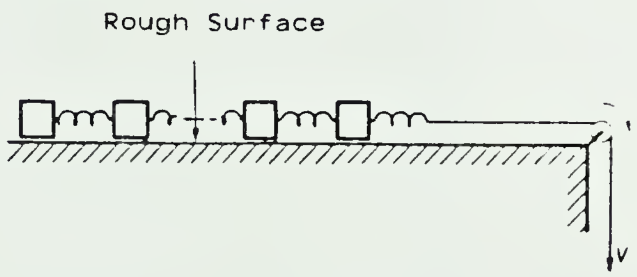

Fig. 5.4 Schematic diagram of the laboratory model.

to(fig. 5.4)the first mass.With this, it is found that small events occur largely at random while large events involving major changes in the elastic potential energy are almost periodic. Between major events, the potential energy of the system increases nearly linearly with times when the intermass springs have equal spring constants. However in case of unequal spring constants this is not so.

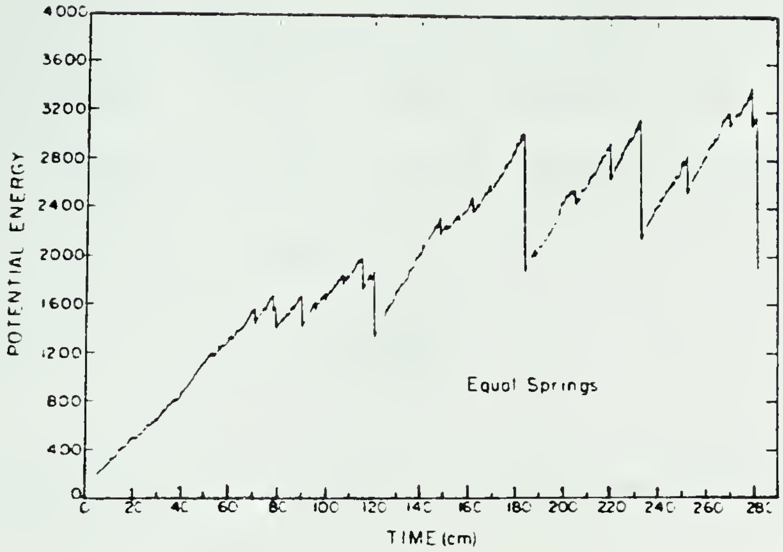

Fig. 5.5 Potential energy as a function of time for Burridge and Knopoff model with all spring equal (Burridge and Knopoff, 1967).

Furthermore, the major events occur at appoximately the same level of the potential energy and involve comparable energy drops (fig. 5.5).

The plot of the frequency of the events as a function

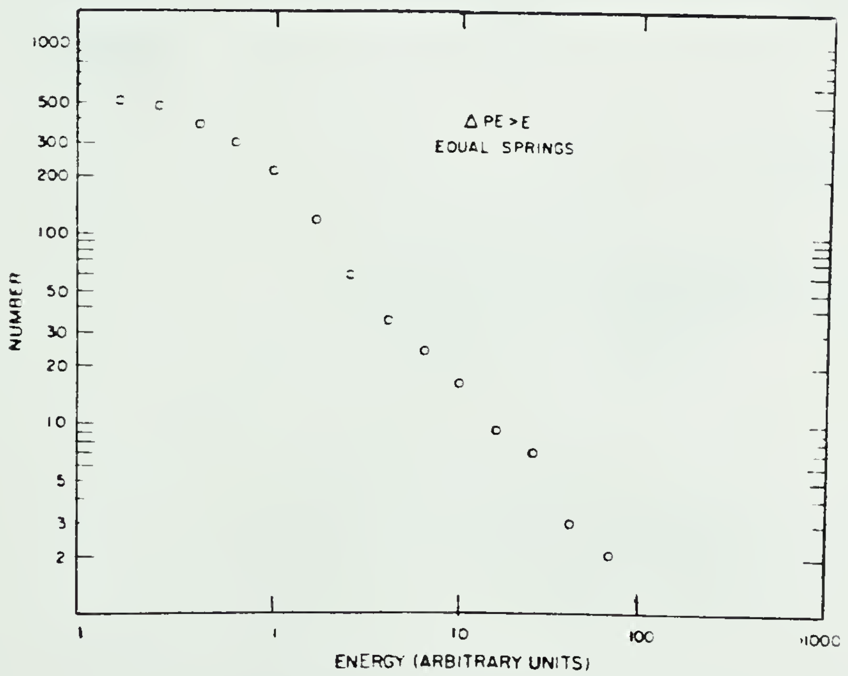

Fig 5.6
Frequency-energy relationship with all spring equal (Burridge and Knopoff, 1967).

of energy released (fig. 5.6) except for the lowest energies fits the equation $\log_{10} N = a - b \log_{10} E$

where N is the frequency of an event occurring with energy release greater than or equal to E. Assuming $\log E = M_{sim}$, where M_{sim} is defined as magnitude of the simulated events, we have

$$\log_{10} N = a - b\, M_{sim}$$

This is analogous to the Gutenberg-Richter frequency magnitude relationship.

Typically in naturally occurring shocks b = 0.4, although there is considerable scatter in the value of b. But in the above model b = 1. Burridge and Knopoff attributed this discrepancy to the one dimensional nature of the model. Furthermore the natural shocks follows a Poisson distribution but in this case some nonPoisson component is present, presumably due to the interaction between adjacent blocks.

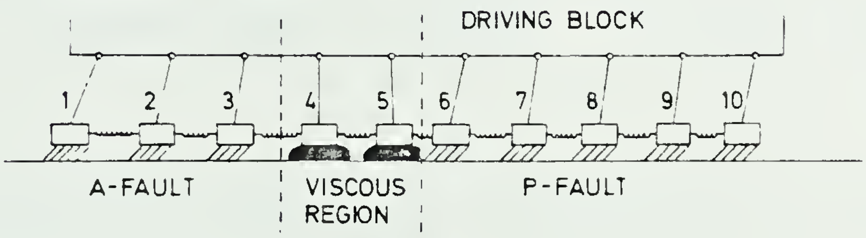

Fig. 5.7 Schematic diagram of the numerical model (Burridge and Knopoff, 1967).

Burridge and Knopoff (1967) also presented results for a one dimensional model by numerical computation. The computational model consists of 10 masses connected by

springs and driven by springs coupled to a moving plate. The 1st three form an auxillary seismic zone, the next two a viscous zone and the last five forms primary seismic zone (fig. 5.7).The viscosity is so high for the middle zone that the friction force is never exceeded by the driving force. Furthermore dynamic friction is assumed to be a function of the velocity of block relative to the friction surface. The assumed friction law is

$$f_i^d(\dot{u}) = -\left(\frac{B}{H}+E\right)\dot{u} \qquad |\dot{u}|<H$$

$$= -\frac{B}{1+A(\dot{u}-H)} - E\dot{u} \qquad \dot{u}>H$$

$$= \frac{B}{1-A(\dot{u}+H)} - E\dot{u} \qquad \dot{u}<-H$$

where H is a value of velocity below which the friction force is linearly related to the velocity. E, B, A are constants incorporating seismic radiation and viscous effects.

The computation shows the movement of the 6th particle starts first followed by motion of the 7th and so on down to the 10th particle. Then motion is reflected back, particle 10 imparts further motion to particle 9 and so on in the reverse order up to the viscous region. This event may be regarded as a main shock. After that there is a quiet period, only particles 4 and 5 move according to a slow adjustment of viscous material following the quake. After

that, the motion of particle 4 triggers a shock in region 1-3. This quake corresponds to an after shock (fig. 5.8).

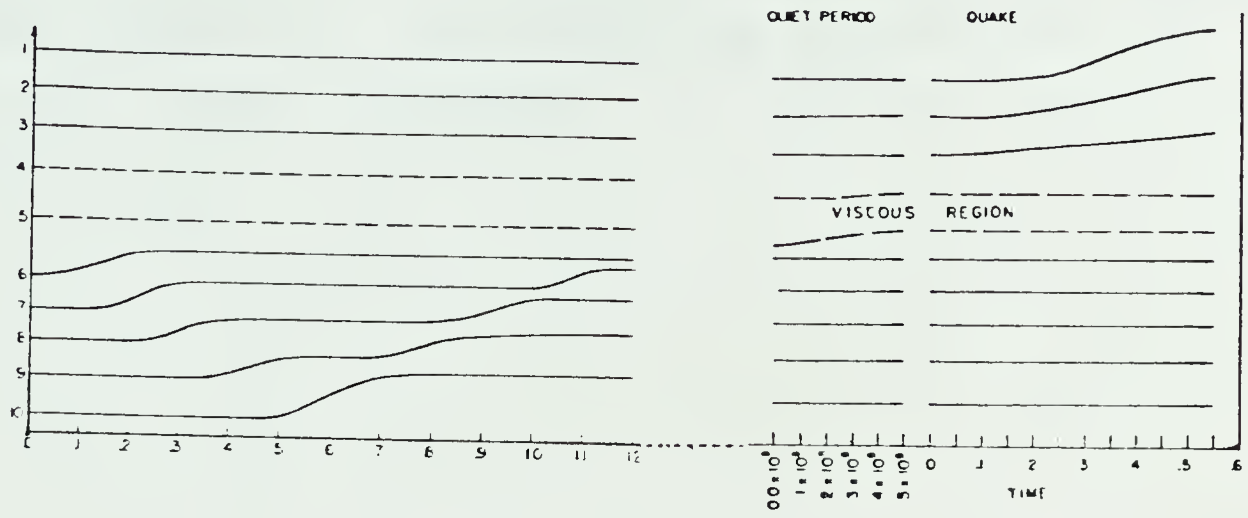

Fig. 5.8

For a number of shallow focus earthquakes which have surface trace of rupture it has been found that there exists a correlation between the magnitude of the shock and the

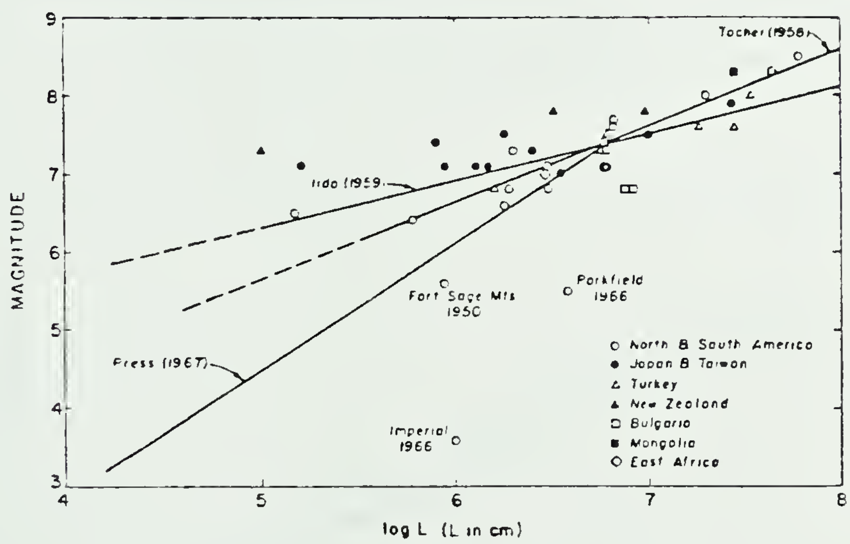

Fig. 5.9 Earthquake magnitude versus fault length.

fault length (fig. 5.9). King and Knopoff (1968) examined this fact in a laboratory model similar to the Burridge and

Knopoff (1967). Assuming that the drop in potential energy of the system is a measure of the magnitude of the earthquake and the number of blocks moved as a measure of fault length (L), they plotted the data and found that there is no linear relationship as observed in natural events (fig. 5.10).

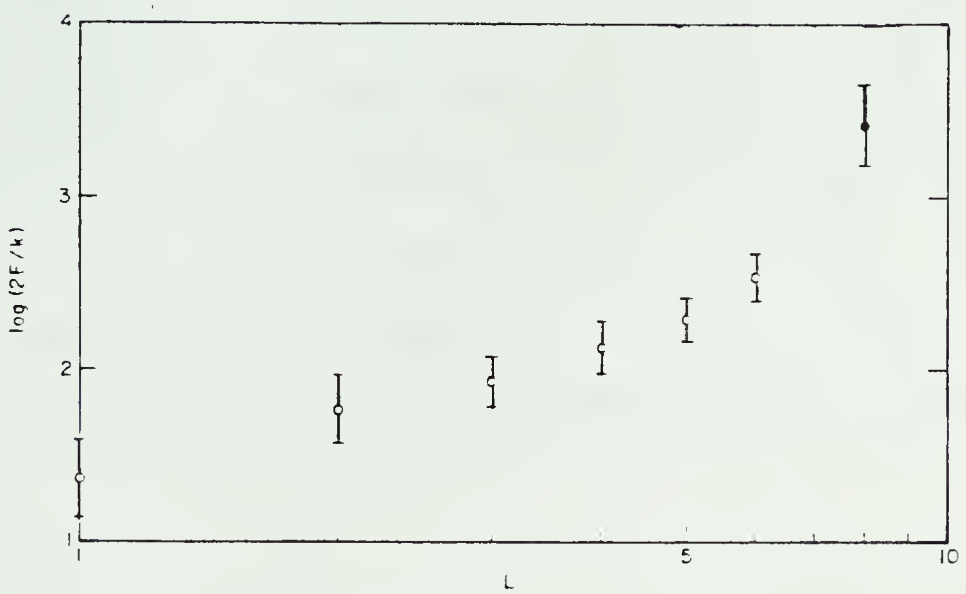

Fig. 5.10 Shock energy versus fault length, solid dot L=8; open circle L<8 (King and Knopoff, 1968).

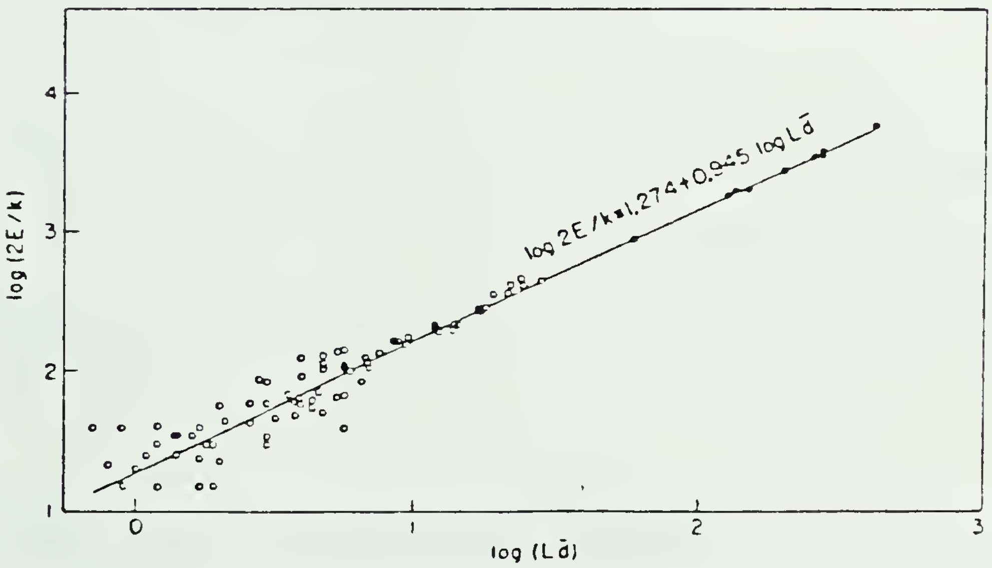

Fig. 5.11 Shock energy versus $L\bar{d}$ (King and Knopoff, 1968).

However, better linear correlation are discovered when $\log E$ is plotted against $\log LD$, $\log LD^2$, and $\log L\bar{d}$, where D and $\bar{d}$ are peak and average displacement respectively. An example of the correlation between E and $L\bar{d}$ is shown fig. 5.11.

Otsuka (1972) extended the Burridge and Knopoff computational model to 2D. The blocks are suspended from an overhead support by leaf springs and are in contact with a moving floor. There are 2000 blocks in a 100X20 grid. Here also the frequency of occurrence of event and energy released (measured by number of blocks moved) shows a relation similar to the Gutenberg-Richter relation (fig 5.12).

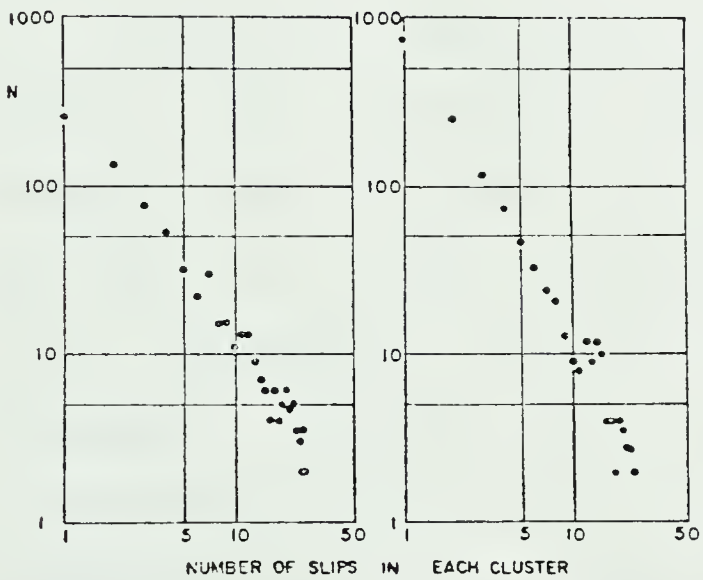

Fig. 5.12
Magnitude-frequency relationship
N is the number of events; the horizontal axis gives numbers of blocks that slips in a given cluster (Otsuka, 1972).

Further large events are found to occur in those regions where seismic activity is anomalously low. This is consistent with the fact that in the period preceeding the

occurrence of a large earthquake, seismic activity is usually low in the region from where a large amount of seismic energy is to be released (fig. 5.13).

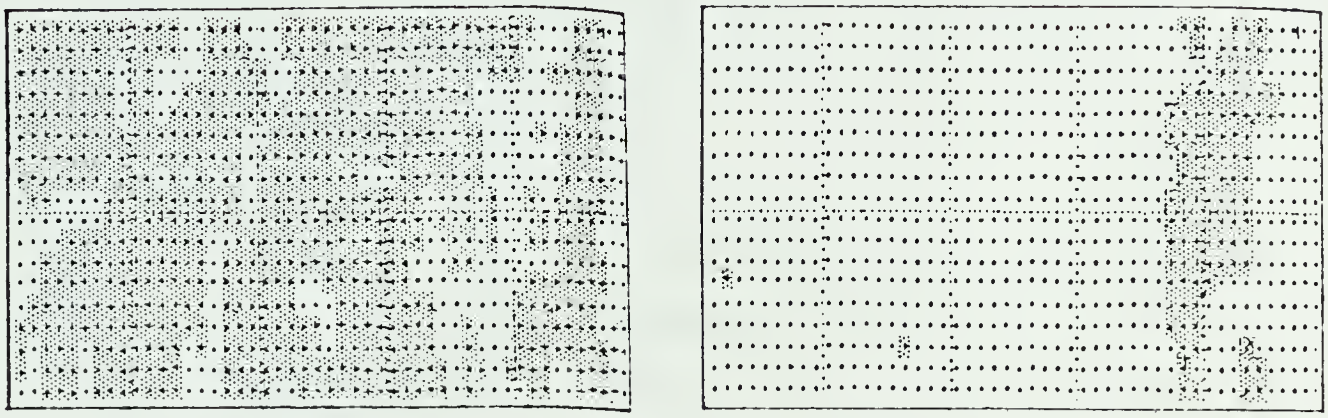

Before mainshock During mainshock

Fig. 5.13 Darkened area shows the region that sliped (Otsuka, 1972).

Dieterich (1972b) also computed earthquake sequences with a one dimensional model similar to Burridge and Knopoff. Four cases are considered in which the coupling spring and friction are as follows (1) elastic spring and time independent friction (2) elastic spring and time dependent friction (3) viscoelastic spring and time independent friction (4) viscoelastic spring and time independent friction. The viscoelastic spring is taken to have some partial stress recovery mechanism in order to produce after-shocks. The time dependent static friction is taken on the basis of result of laboratory experiments and is given by the equation 5.1.

In all cases, the frequency with which a block moves is related to its static friction; blocks with low friction moves more frequently than those with high friction(fig.5.14

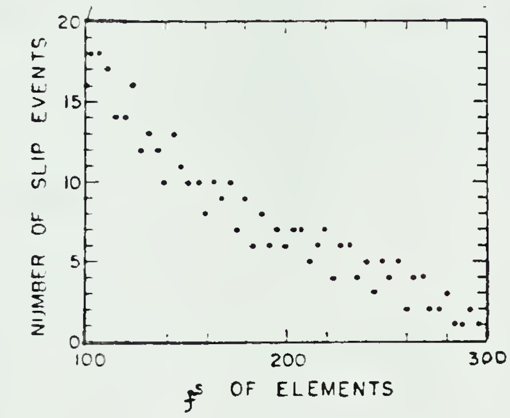

Fig. 5.14
Correlation between the frictional strength of the block and the number of times the block slipped (Dieterich, 1972b).

). In the first three cases no after-shocks are produced, even when extreme values for the parameter are chosen that

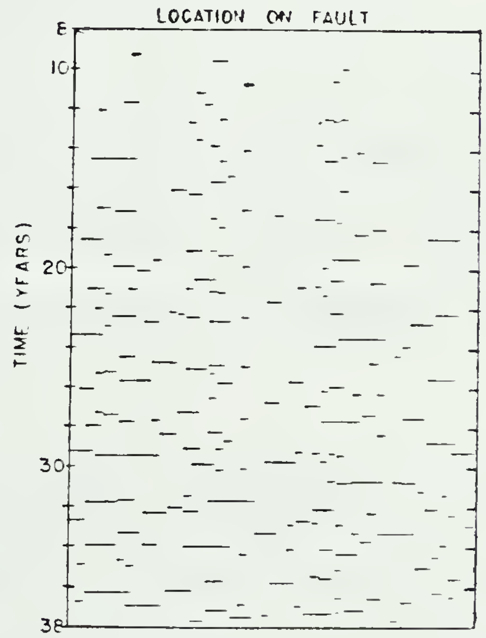

Fig. 5.15
Plot ot the earthquakes in the model with perfect elasticity and simple friction. There is no distinction between mainshock and aftershock (Dieterich, 1972b).

give large stress recovery following the event. For example a plot of the first case is reproduced (fig 5.15). There is no distinction between the main shocks and after-shocks. The last case, viscoelastic element with time dependent

friction, shows an after-shock sequence following the main-shock. These occurs on the same segment affected by main-shock. Further the duration of the after-shock directly related to the magnitude of the mainshock. Large earthquakes have after-shocks sequences that last longer than those of

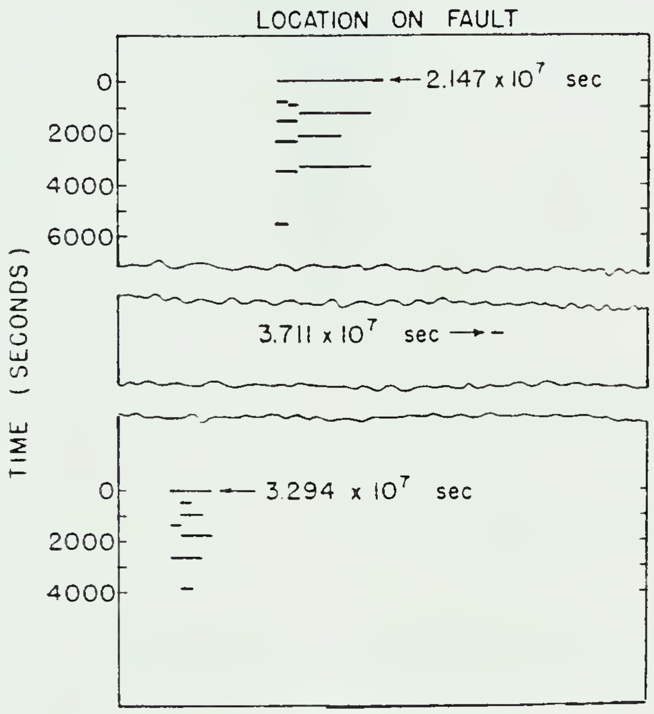

Fig. 5.16
Plot of earthquake for time dependent friction and visco-elasticity. Arrows are marked against mainshocks (Dieterich, 1972b).

smaller earthquakes. Also the frequencies of main-shocks and after-shocks are easily distinguishable (fig. 5.16). Dieterich (1973) has also developed numerical schemes for two- and three-dimensional simulation.

Cohen (1977) stimulated earthquake sequences on the basis of Dietrich's (1972b) model and concluded that seismic gaps are more likely to occur when there are large variations of elastic or frictional parameters. If the parameters are homogeneous from block to block the simulated earthquake are periodic and successive events propagate throughout the fault. With the increase in the spring constant of the driving spring compared to the connecting

spring, the length of shocks decreases. Furthermore there is a correlation between the displacement of the largest after-shock and those of the main-shock (fig. 5.17).

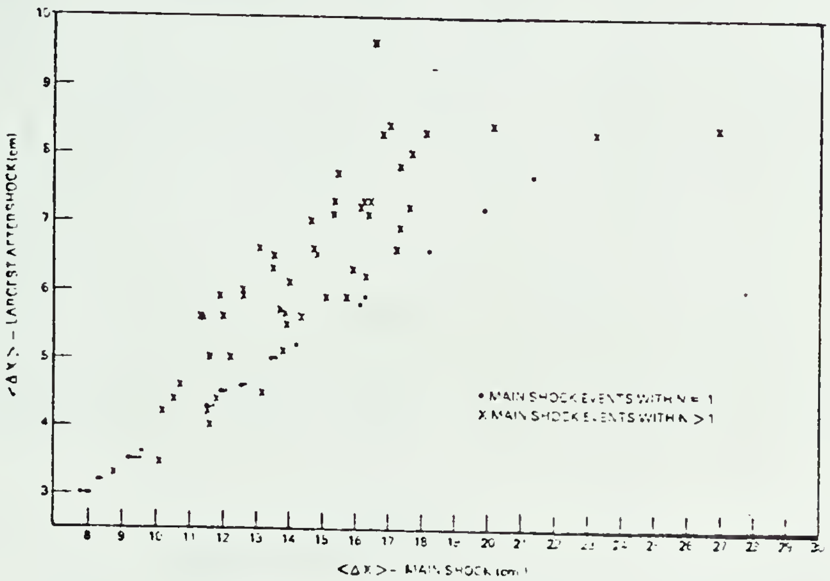

Fig. 5.17 Plot between displacement of the mainshock and the largest aftershock (Cohen, 1977).

Recently Rundle & Jackson (1977) have re-examined the Burridge and Knopoff model employing 20 blocks with elastic as well as anelastic coupling. For the elastic model he took three different friction laws. In the first case the static friction varies violently from block to block (maximum to minimum is 30:1) while dynamic friction lies at constant value much below the lowest value of static friction. In the second case static friction changes very smoothly and dynamic friction is 0.8 times static friction. In the third case the dynamic friction is held constant and static friction changes by constant amount over the dynamic friction from block to block. For the anelastic model, static friction is assumed to be stress as well as time dependent and static friction f^s decreases at a rate

proportional to the amount by which the stress causing motion exceeds some value of friction f^{sd}

$$\frac{df^s}{dt} = -\frac{1}{\tau}\left[\sigma(t) - f^{sd}\right]$$

where τ is a constant and $\sigma(t)$ is the stress acting on the block.

In all these cases they found that the frequency-magnitude relationship for stimulated earthquake

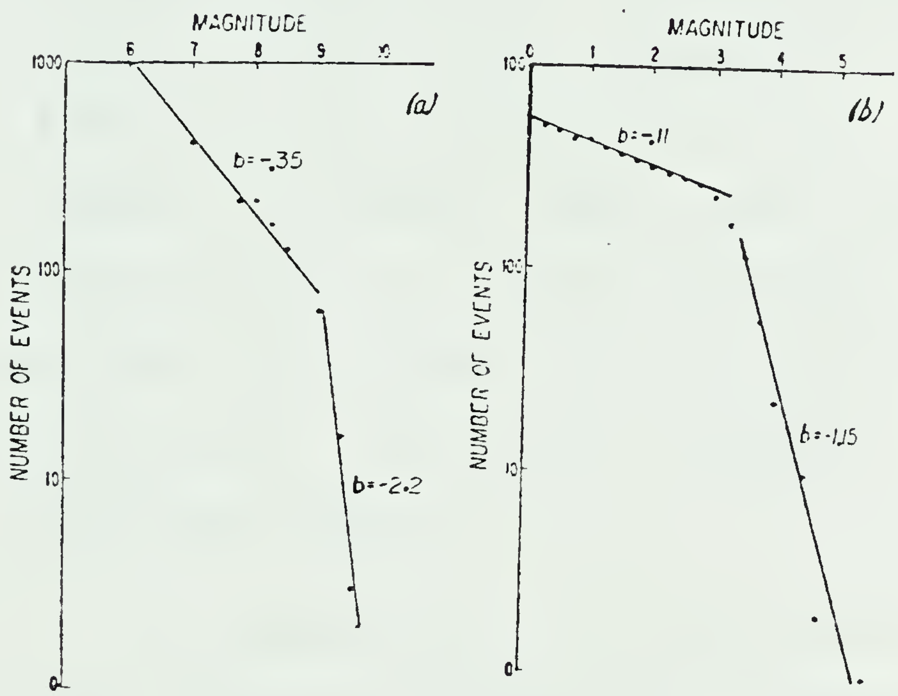

Fig. 5.18
Frequency-magnitude relationship
(Rundel and Jackson, 1977)
(a) Elastic model
(b) Anelastic model

is not consistent with that of natural earthquake (fig. 5.18). With the different value of elastic parameter the situation does not improve. So they have concluded that linear behaviour of magnitude-frequency relationship is not an immutable law but rather is dependent on the mechanical properties of the fault, although in some real earthquakes, magnitude frequency relationship is similar to their result.

King (1975) has pointed out that if the breaking strength is considered to be finite so the model can store only a finite amount of strain energy, then there will be a decrease in the relative number of large event, hence the frequency-magnitude relationship may not be linear.

With the anelastic model it is possible to simulate aftershock sequences. Here if the dynamic friction is greater than f^{sd}, the stress drop during the first rupture is small, and the stress $\sigma(t)$ remains large, causing decrease in frictional strength. Since friction is then reduced while stress remains high, aftershocks may occur. Moreover, the aftershocks will not be confined only to the region of primary shock, since the stress induced failure may also occur in a region adjacent to that which ruptured during the primary event (this border region having been stressed by the elastic elements coupling it to the displaced region).

On examination of the variation in the frequency of the time intervals between events, some nonPoisson components in this distribution of interevent periods are found. Rundle and Jackson attributed these to the interaction between adjacent events. The motion of one block alters the compression of the spring connecting it to the neighbouring block, thus altering the stress and the time at which the stress overcomes the frictional resistance.

None of the models discussed so far have accounted for healing or stopping of the slippage. Moreover, due to the discrete nature of the models there is fictitious spatial variation of stress, so that any calculation for stopping is unreliable with these models. A realistic picture can be had if a continuous model is considered. Knopoff et al. (1973) have developed a continuum model by letting the interblock distance of the Burridge and Knopoff discrete model to approach zero. They thus formulated an one-dimensional unilateral rupture problem. They showed that if the static friction increases or the difference between the driving stress and dynamic friction decreases sufficiently in the region ahead of the rupture tip, the rupture can stop. Thus some variation in either friction or stress appears to be necessary to stop the rupture. Israel and Nur (1979) have studied the effect of strongly variable stress and frictional strength and concluded that such a heterogeneity is closely linked to the stopping phase of the fault motion.

Mikumo and Miyatake (1978,79) have investigated the earthquake sequence on a three dimensional block model with non-uniform friction and spring constants, subjected to a time dependent shear stress. They found that after-shock with high stress drop occur in and around the unruptured part of regions on which main-shock has already occured, while those with low stress drop take place successively in spaced regions so as to fill the gaps which were not ruptured during main-shock. The main-shocks take place

successively in adjacent unruptured regions and sometimes show slow-speed migrations. Also they found a good linear relations in logarithmic scale for source area versus frequency and seismic moment versus frequency of the generated after-shocks.

The major contribution of the simulation studies has been in the understanding of the rupture propagation along a fault, in developing correlations among source parameters, and in explaining the interplay among foreshocks, mainshocks, aftershocks and creep. It appears that the simulation studies should be extended to two- and three-dimensional viscoelastic systems, possibly with multiple faults. With complicated rheological models, the greater number of adjustable parameters may give freedom to simulate completely on computer a natural earthquake sequence. This may be useful for earthquake predictions. Moreover, there is no direct link between movements of the blocks and far field radiation in the simulation models developed so far. So a synthesis of techniques, such as a combination of a sliding block description of rupture with a dislocation theory description of the far field effect might prove fruitful.

6. RECENT TRENDS IN THE SOURCE THEORY

In the recent past studies in the source theory have been directed to develop more realistic models by taking into account the layering in the source region, effects of the free surface, and anelasticity of the medium. Also there have been attempts to account for the energy balance during faulting.

With the work of Lee and Teng (1973) on the radiation pattern for P and SV waves due to various point sources embedded in a flat multilayered medium, the study on the effect of layering started. The mathematical tools developed by Ben-Menahem and Vered (1973) and Helmberger (1974) where applied by Langston and Helmberger (1975) and Bouchon (1976) to shallow dislocation sources in a layered half space, and they obtained analytical expressions for the displacements. To synthesize the strong ground motions produced by a propagating dislocation embedded in a layered medium, Heaton and Helmberger (1977,1978) modeled the source as a distributed set of shear dislocation points and computed the individual responses using generalized ray theory. Bouchon(1977,79) developed an exact discretization scheme for the elastic fields generated by such a fault, and the seismograms obtained were then combined to yield the space and time dependence of the ground motion (Bouchon, 1980).

The results showed the strong directivity effects on the propagating rupture. Large surface displacements and high-frequency motions were confined to a narrow zone around the fault and to the region which extends beyond the source along the trend of the fault. SH and Love waves were the dominant contributions to the ground shaking. The vertical displacement were small but exhibited high frequency content. The presence of low-velocity surface layer had a very severe effect on the amplitude and duration of the ground shaking.

The effect of a free surface on seismograms has been examined by Israel and Kovach (1977) and Langston (1978). They found that depending on source orientation, depth, and time function, errors in moment and corner frequency determination may be large due to neglecting the free surface.

A few efforts have been made to study earthquakes in the context of a more general constitutive relation such as Budiansky and Amazigo (1976) and Burridge (1977). They have assumed a model in which the vicinity of the a vertical fault plane is represented by a Maxwell viscoelastic half space.

In some of the earthquakes, permanent elevation changes in the vicinity of the focus have occured. This suggests that during faulting work is done against gravitational forces. Several authors (Meister et al.(1968), Jungels and

Frazier (1972)) have noted that the work done against gravity in a dip-slip faulting appears to much larger than usual estimates of energy release in the faulting (Gutenberg-Richter energy-magnitude formula), with the implication that the conventional measure of the earthquake energy is a gross under-estimate. This difficulty was resolved by Dahlen (1977), who defined an earthquake by specifying on the fault surface a jump discontinuity in tangential displacement which expands within a uniformly rotating, self-gravitating earth model.The total amount of energy released by such an idealized earthquake is the sum of three distinct quantities: kinetic energy of rotation, gravitational potential energy and thermodynamic elastic internal energy. Although, the total energy release is in general considerably smaller than any of its three individual constituents, with this model the energy release rate is simply

$$\int (\sigma^0_{ij} + \sigma_{ij})/2 \; u_i \, dS_j$$

where σ^0_{ij} is the ambient stress before faulting, σ_{ij} and u_i are the stress change and displacement associated with the faulting and integral is over fault surface.

And the expression for the work done against gravity is

$$-\int \rho g_i u_i \, dV$$

where g_i is the acceleration due to gravity, and the integral is over the entire volume of the body.

Dahlen pointed out that although the gravitational energy change may be several orders of magnitude greater than the energy release, this large change in the gravitatioal energy is approximately compensated for by a similar change in elastic energy initially stored in the Earth. Thus the actual energy released (i.e., seismic energy, workdone against friction, new surface energy) is rather small difference between these two large potential energy changes.Savage and Walsh (1978) have also concluded the same.

The present state of art in the source theory can give us the seismic motion due to a given condition of stress and material properties, but in order to have a realistic prediction of the earthquake occurrence and particularly foreshocks, aftershocks, and other related phenomena, the actual distribution in space of tectonic stress field and material properties in the epicentral region should be considered. And here is the challenge, neither those distributions are known precisely nor analytical techniques are developed to tackle such a heterogeneous distribution.

BIBLIOGRAPHY

Achenbach, J. D., On dynamic effect in brittle fracture, In: S. Nemat-Nasser (Editor), Mechanics Today, Pergamon Press, New York, 1, 1-57, 1974.

Aki, K., Scaling law of seismic spectrum, Jour. Geophys. Res., 72, 1217-1231, 1967.

Aki, K., and P. G. Richards, Quantitative Seismology theory and methods, Freeman, San Francisco, 1980.

Alterman, Z. S., and J. Aboudi, Source finite extent, applied force and couple in an elastic half space, Geophys. Jour. Roy. Astr. Soc., 21, 47-64, 1970.

Andrews, D. J., Plain strain models of earthquakes that stops, Bull. Seism. Soc. Am., 65, 163-182, 1975.

Andrews, D. J., Rupture velocity of plain-strain shear cracks, Jour. Geophys. Res., 81, 5679-5687, 1976.

Archambeau, C. B., General theory of elasto-dynamic source fields, Rev. Geophys., 6, 241-288, 1968.

Archambeau, C. B., Development in seismic source theory, Rev. Geophys. Space Phys., 13, 304-306, 1975.

Atkinson, C., and J. D. Eshelby, The flow of energy into the tip of moving crack, Int. Jour. Fract. Mech., 4, 3-8, 1968.

Backus, G. E., Interpreting the seismic gult moments of total degree two or less, Geophys. Jour. Roy. Astr. Soc.

51, 1-25, 1977a.

Backus, G. E., Seismic source with observable gult moment of spatial degree two, Geophys. Jour. Roy. Astr. Soc., 51, 27-45, 1977b.

Backus, G. E., and M. Mulcahy, Moment tensors and other phenomenological descriptions of seismic sources. I Continuous displacement, Geophys. Jour. Roy. Astr. Soc., 46, 341-361, 1976a.

Backus, G. E., and M. Mulcahy, Moment tensors and other phenomenological description of seismic sources. II Discontinous displacement, Geophys. Jour. Roy. Astr. Soc., 47, 301-329, 1976b.

Balakina, L. M., E. F. Savarensky, and A. V. Vvedenskaya, On determination of earthquake mechanism, Phys. Chem. Earth, , 4, 221-238, 1961.

Barenblatt, G. I., The mathematical theory of equilibrium cracks in brittle fracture, Advan. Appl. Mech., 7,55-129, 1962.

Ben-Menahem, A., Radiation of seismic surface wave from a finite moving source, Bull. Seism. Soc. Am., 51, 401-435, 1961.

Ben-Menahem, A., Radiation of seismic body waves from a finite moving source in the earth, Jour. Geophys. Res., 67, 345-350, 1962.

Ben-Menahem, A., and S. J. Singh, Computation of models of elastic dislocation in the earth, In: B. A. Bolt (Editor), Methods in computational physics, Academic Press, New York, 12, 299-375, 1972.

Ben-Menahem, A., and M. N. Toksoz, Source-mechanism from specta of long period seismic surface waves, Jour. Geophys. Res., 68, 5207-5222, 1963.

Ben-Menahem, A., and M. Vered, Extension and interpretation of Cagniard-Pekeris method for dislocation sources, Bull. Seism. Soc. Am., 63, 1611-1636, 1973.

Bilby, B. A., and J. D. Eshelby, The dislocation theory of fracture, In: H. Liebowitz (Editor), Fracture an Advance Treatise, Academic press, New York, 1, 100-183, 1968.

Bouchon, M., Teleseismic body radiation from a seismic source in a layered medium, Geophys. Jour. Roy. Astr. Soc., 47, 515-530, 1976.

Bouchon, M., Discrete wave number representation of elastic wavefields in three-space dimension, Jour. Geophys. Res., 84, 3609-3614, 1979.

Bouchon, M., The motion of the ground during the earthquake. 1. The case of a strike-slip fault, Jour. Geophys. Res., 85, 356-366, 1980.

Bouchon, M., and K. Aki, Discrete wave-number repesentation of seismic source wave fields, Bull. Seism. Soc. Am., 67, 259-277, 1977.

Brace, W. F., and J. D. Byerlee, Stick-slip as a mechanism of earthquakes, Science, 153, 990-992, 1966.

Brune, J. N., Tectonic stress and spectra of seismic shear waves from earthquakes, Jour. Geophys. Res., 75, 4997-5009, 1970.

Budiansky, B., and J. C. Amazigo, Interaction of fault slip

and lithosphere creep, Jour. Geophys. Res., 81, 4897-4900, 1976.

Burridge, R., The numerical solution of certain integral equations with non-integrable kernals arising in the theory of crack propagation and elastic wave diffraction, Phil. Trans. Roy. Soc., A265, 353-381, 1969.

Burridge, R., A repetitive earthquake source model, Jour. Geophys. Res., 82, 1663-1666, 1977.

Burridge, R., and L. Knopoff, Body force equivalent for seismic dislocations, Bull. Seism. Soc. Am., 54, 1875-1888, 1964.

Burridge, R., E. R. Lapwood, and L. Knopoff, First motion from seismic sources, Bull. Seism. Soc. Am., 54, 1889-1913, 1964.

Burridge, R., and L. Knopoff, Model and theoretical seismicity, Bull. Seism. Soc. Am., 57, 341-371, 1967.

Burridge, R., G. Conn, and L. B. Freund, The stability of a rapid mode II shear crack with finite cohesive traction, Jour. Geophys. Res., 84, 2210-2222, 1979.

Byerlee, J. D., The mechanics of stick-slip, Tectophysics, 9, 475- 486, 1970.

Cohen, S. C., Computer simulation of earthquakes, Jour. Geophys. Res., 82, 3781-3796,, 1977.

Cohen, S. C., The viscoelastic stiffness model of seismicity, Jour. Geophys. Res., 83, 5425-5431, 1978.

Cohen, S. C., Numerical and laboratory simulation of fault motion and earthquake occurence, Rev. Geophys. Space Phys., 17, 61-72, 1979.

Dahlen, F. A., The balance of energy in earthquake faulting, Geophys. Jour. Roy. Astr. Soc., 48, 239-251, 1977.

de-Hoop, A. T., Representation theorm for the displacement in an elastic solid and their applicationto elastodynamic diffraction theory, Doctral dissertation, Delft, 1958.

Dieterich, J. H., Time-dependent friction in rocks, Jour. Geophys. Res., 77, 3690-3697, 1972a.

Dieterich, J. H., Time-dependent friction as a possible mechanism for aftershocks, Jour. Geophys. Res., 77, 3771-3781, 1972b.

Dieterich, J. H., A deterministic near field source model, Proc. World Conf. Earthquake Eng. 5th, pap. no. 301, 13, 1973.

Dieterich, J. H., Modeling of rock friction. 1. Experimental result and constitutive equation, Jour. Geophys. Res., 84, 2161-2168, 1979.

Fossum, A. F., and L. B. Freund, Nonuniformly moving shear crack model of a shallow focus earthquake mechanism, Jour. Geophys. Res., 80, 3343-3347, 1975.

Freund, L. B., Energy flux into the tip of an extending crack in an elastic field, Jour. of Elasticity, 2, 341-348, 1972.

Freund, L. B., The analysis of elastodynamic crack tip stress fields, In: S. Nemat-Nasser (Editor), Mechanics Today, Pergamon Press, 3, 55-92, 1976.

Freund, L. B., The mechanics of dynamic shear crack propagation, Jour. Geophys. Res., 84, 2199-2209, 1979.

Griffith, A. A., The phenomena of rupture and flow in solids, Phil. Trans. Roy. Soc., A221, 163-198, 1920.

Haskell, N. A., Radiation patterns of Rayliegh waves from a fault of arbitrary dip and direction of motion in a homogeneous medium, Bull. Seism. Soc. Am., 53, 377-393, 1963.

Haskell, N. A., Total energy and energy spectral density of elastic wave radiation from propagating faults, Bull. Seism. Soc. Am., 54, 1811-1841, 1964.

Haskell, N. A., Total energy and energy spectral density of elastic wave radiation from propagating fault. Part II. A statistical source model, Bull. Seism. Soc. Am., 56, 125-140, 1966.

Haskell, N. A., Elastic displacements in the near-field of a propagating fault, Bull. Seism. Soc. Am., 59, 865-908, 1969.

Heaton, T. H., and D. V. Helmberger, A study of the strong ground motion of the Borrego Mountain, California, earthquake, Bull. Seism. Soc. Am., 67, 315-330, 1977.

Heaton, T. H., and D. V. Helmberger, Predictability of strong ground motion in the Imperial Valley: Modeling the M4.9, November 4, 1976 Brawley earthquake, Bull. Seism. Soc. Am., 68, 31-48, 1978.

Helmberger, D. V., Generalized ray theory for shear dislocations, Bull. Seism. Soc. Am., 64, 45-64, 1974.

Hirasuwa, T., and W. Stauder, On the seismic body waves from a finite moving source, Bull. Seism. Soc. Am., 55, 237-262, 1965.

Honda, H., Earthquake mechanism and seismic waves, Geophys. Notes, 15 suppl., Tokyo Univ., 1962.

Husseini, M. I., D. B. Jovanovich, M. J. Randall, and L. B. Freund, The fracture energy of earthquakes, Geophys. Jour. Roy. Astr. Soc., 43, 367-385, 1975.

Ida, Y., Stress concentration and unsteady propagation of logitudinal shear cracks, Jour. Geophys. Res., 78, 3418-3429, 1973.

Irwin, G. R., Fracture, In: S. Flugge (Editor), Handbuch der Physik, Springer-Verlag, Berlin, 6, 551-590, 1958.

Israel, M., and R. L. Kovach, Near-field motions from a propagating strike-slip fault in an elastic half-space, Bull. Seism. Soc. Am., 67, 977-994, 1977.

Israel, M., and A. Nur, A complete solution of a one-dimensional propagating fault with non uniform stress and strength, Jour. Geophys. Res., 84, 2223-2234, 1979.

Jaeger, J. C., and N. G. W. Cook, Fundamentals of Rock Mechanics, Halsted, London, 1976.

Johnson, L. R., Seismic source theory, Rev. Geophys. Space Phys., 17, 328-336, 1979.

Jungel, P. H., and G. Frazier, Calculation of prestress, stress drop and energy release in shallow earthquake, E.O.S. Trans. Am. Geophys. Union, 53, 119, 1972.

Keilis-Borok, V. I., An estimation of the displacement in an earthquake source and of source dimensions, Ann. Geophys., 12, 205-214, 1959.

King, C. Y., Model seismicity and faulting parameters, Bull. Seism. Soc. Am., 65, 245-259, 1975.

King, C. Y., and L. Knopoff, Model seismicity: Rupture parameters, stress, and energy relations, Jour. Geophys. Res., 73, 1399-1406, 1968.

Knopoff, L., J. O. Moulton, and R. Burridge, The dynamics of one dimensional fault in a presence of friction, Geophys. Jour. Roy. Astr. Soc., 35, 169-184, 1973.

Knopoff, L., and M. J. Randall, The compensated linear-vector dipole: a possible mechanism for deep earthquakes, Jour. Geophys. Res., 75, 4957-4963, 1970.

Kostrov, B. V., Unsteady propagation of longitudinal shear cracks, Jour. Appl. Math. Mech., 30, 1241-1248, 1966.

Kostrov, B. V., On the crack propagation with variable velocity, Int. Jour. Fract. Mech., 14, 47-56, 1975.

Kostrov, B. V., and L. V. Nikitin, Some general problem of mechanics of brittle fracture, Arch. Mech. Stos., 22, 749-776, 1970.

Lamb, H., On the propagation of tremors at the surface of an elastic solid, Phil. Trans. Roy. Soc., A203, 1-42, 1904.

Langston, C. A., Moments, corner frequencies, and the free surface, Jour. Geophys. Res., 83, 3422-3426, 1978.

Langston, C. A., and D. V. Helberger, A procedure for modeling shallow dislocation sources, Geophys. Jour. Roy. Astr. Soc., 42, 117-130, 1975.

Lawn, B. R., and T. R. Wilshaw, Fracture of Brittle Solids, Cambridge university Press, Cambridge, 1975.

Lee, T. C., and T. L. Teng, Polar radiation patterns of P and SV waves in a multilayered medium, Bull. Seism. Soc. Am., 63, 529-547, 1973.

Logan, J. M., Friction in rocks, Rev. Geophys. Space Phys., 13, 358-361, 1975.

Madariaga, R., Dynamics of an expanding circular fault, Bull. Seism. Soc. Am., 64, 163-182, 1976.

Madariaga, R., High frequency radiation from crack (stress drop) model of earthquake faulting, Geophys. Jour. Roy. Astr. Soc., 51, 625-651, 1977.

Maruyama, T., On the force equivalents of dynamic elastic dislocation with refrence to the earthquake mechanism, Bull. Earthq. Res. Inst. Tokyo, 41, 467-486, 1963.

Meister L. J., R. O. Burford, G. A. Thompson, and R. L. Kovach, Surface strain change and strain energy release in Dixie Valley-Fairview Peak area, Nevada, Jour. Geophys. Res., 73, 5981-5994, 1968.

Mikumo, T. and T. Miyatake, Dynamical rupture process on three-dimensional fault with non-uniform friction and

near field seismic waves, Geophys. Jour. Roy. Astr. Soc., 54, 417-438, 1978.

Mikumo, T., and T. Miyatake, Earthquake sequence on a frictional fault model with non-uniform strength and relaxation times, Geophys. Jour. Roy. Astr. Soc., 59, 497-522, 1979.

Mott, N. F., Fracture of metals: Some theoretical considerations, Engineering, 165, 16-18, 1948.

Nur, A., Non-uniform friction as a physical basis for earthquake mechanics, Pure Appl. Geophys., 116, 964-991, 1978.

Nur, A., and P. Schultz, Fluid flow and faulting. 2. A stiffness model for seismicity, in Proceedings of the Conference on Tectonic Problems of San Andreas Fault System, Stanford, 1973, Stanford University press, Stanford, Calif., 405-416, 1973.

Otsuka, M., A simulation of earthquake occurrence, Phys. Earth Plant. Interiors, 6, 311-315, 1972.

Randall, M. J., Multipolar analysis of the mechanism of deep focus earthquakes, In: B. A. Bolt (Editor), Method in computational physics, Academic press, New York, 12, 267-298, 1972.

Richards, P. G., The dynamic field of a growing plane elliptical shear crack, Int. Jour. Solid Structures, 9, 843-861, 1973.

Richards, P. G., Dynamic motion near an earthquake fault: a three -dimensional solution, Bull. Seism. Soc. Am., 66, 1-32, 1976.

Rundel, J. B., and D. D. Jackson, Numerical simulation of earthquake sequences, Bull. Seism. Soc. Am., 67, 1363-1377, 1977.

Savage, J. C., The effect of rupture velocity upon seismic first motions, Bull. Seism. Soc. Am., 55, 263-275, 1965.

Savage, J. C., Radiation from realistic model of faulting, Bull. Seism. Soc. Am., 56, 577-592, 1966.

Savage, J. C., and J. B. Walsh, Gravitational energy and faulting, Bull. Seism. Soc. Am., 68, 1613-1622, 1978.

Singh, S. J., A. Ben-Menahem, and M. Vered , A unified approach to the representation of seismic sources, Proc. Roy. Soc. Lond., A331, 1973.

Steketee, J. A., Some geophysical application of the elasticity theory of dislocations, Canad. Jour. Phys., 36, 1168-1198, 1958.

Volterra, V., Ann. sci. ecole. norm. superieure, Ser. 3, 24, 401, 1907.

Whitehead, J. A., and R. F. Gans, A new theoretically tractable earthquake model, Geophys. Jour. Roy. Astr. Soc., 39, 11-28, 1974.